SOUND RADIATION RESPONSES AND ACOUSTIC BEHAVIOR OF SANDWICH PANEL

A Thesis

Submitted to the Faculty of Graduate Studies and Research in Partial Fulfillment of the Requirements for the Degree of

Master of Applied Science

In

Industrial Systems Engineering

University of Regina

By

Luyao Wang

Regina, Saskatchewan

March, 2019

UNIVERSITY OF REGINA

FACULTY OF GRADUATE STUDIES AND RESEARCH

SUPERVISORY AND EXAMINING COMMITTEE

Luyao Wang, candidate for the degree of Master of Applied Science in Industrial Systems Engineering **,** has presented a thesis titled, ***Sound Radiation Responses and Acoustic Behavior of Sandwich Panel ,*** in an oral examination held on March 19, 2019. The following committee members have found the thesis acceptable in form and content, and that the candidate demonstrated satisfactory knowledge of the subject material.

External Examiner:	Dr. Nader Mobed, Department of Physics
Supervisor:	Dr. Liming Dai, Industrial Systems Engineering
Committee Member:	Dr. Amr Henni, Industrial Systems Engineering
Committee Member:	Dr. Mehran Mehrandezh, Industrial Systems Engineering
Chair of Defense:	Dr. Yee-Chung Jin, Environmental Systems Engineering

ABSTRACT

Sandwich structures with decent sound insulation and absorption properties have been widely used in the engineering fields such as aerospace engineering, marine engineering and civil and construction engineering. Investigations on the acoustic behavior of sandwich structures is of practical importance, not only for engineers but to researchers in the field. A numerical study of the vibro-acoustic and sound transmission loss (STL) of an aluminum honeycomb core sandwich panel with fabric-reinforced graphite (FRG) composite face sheets is performed in the present research. The honeycomb sandwich structure, faced with an FRG composite face sheet, has acoustic advantages over other types of sandwich structures commonly used in the field. The effects of different boundary conditions and geometric properties of the FRG faced honeycomb structure on the stiffness of the structure are evaluated. The effects of the stiffness on the acoustic performance of the structure are investigated.

Truss core sandwich panels filled with sound absorbing materials are also studied numerically for the panels' vibration responses and STL behavior. The performances of a polyurethane (PUF)-foam-filled truss core sandwich panel and a wood-board-filled truss core sandwich panel are compared. The wood based sandwich panel shows advantages with compatible acoustic performance and environmental-friendly characteristics over the PUF foam panel. The acoustic behavior of the wood-based porous media, with varying airflow properties, are investigated. The most significant factor affecting the vibro-acoustic responses of the panel are identified. The wood-based-porous-medium-filled truss core sandwich panel with various face sheet materials are analyzed. A truss core

sandwich panel is designed with the optimal combination of wood-board and face sheet materials.

Numerical models, based on the sandwich theory, are established based on the assumption the sandwich core is an orthotropic structural layer. The radiated sound power from the panel is quantified with the Rayleigh integral method. A random diffuse field is used as an incident sound source and is derived with the finite element method using ACTRAN. The numerical results generated with the implementation of the models are validated with experimental data available in the literature. The findings provide guidance for selecting and designing honeycomb core and truss core sandwich panels with decent acoustic properties for engineering applications. The developed approach presents practical significance for quantitatively evaluating and designing sandwich panels with high efficiency and effectiveness, when the acoustic and vibrational performance of the panels need to be considered.

.

ACKNOWLEDGEMENTS

The author would like to express her sincere appreciation to her supervisor, Dr. Liming Dai, for his patient guidance, expertise, and continuous support throughout the process of her Master of Applied Science program. The invaluable advice, encouragement, and financial support were important to the completion of this research.

The author also wishes to acknowledge the Natural Sciences and Engineering Research Council of Canada (NSERC) for financial support, and the Faculty of Graduate Studies and Research at the University of Regina for financial support in the form of Graduate Scholarships.

The author is highly appreciative of the advice from the committee members and would like to thank all her colleagues in her research group.

DEDICATION

Special thanks to my dear parents, brother and my fiancé for their continuous encouragement and unconditional support.

TABLE OF CONTENTS

ABSTRACT ……1

ACKNOWLEDGEMENTS 3

DEDICATION ……4

TABLE OF CONTENTS 5

CHAPTER1 INTRODUCTION 8

1.1 Background 8

1.2 Research subjects and contributions 9

CHAPTER 2 LITERATURE REVIEW 12

2.1 Sound insulation concepts 12

2.2 Sound insulation formula 15

2.3 The principle of sound insulation 16

2.3.1 The principle of sound insulation for a single-panel structure 16

2.3.2 The principle of sound insulation for single-panel structures 19

2.3.3 The principle of sound insulation for single-panel structure 22

CHAPTER 3 VIBRO-ACOUSTIC RESPONSES OF A SANDWICH PANEL WITH ALUMINUM HONEYCOMB CORE AND FABRIC REINFORCED GRAPHITE FACHINGS 23

3.1 Introduction 23

3.2 Model establishment and numerical methodology 28

3.3 Validation studies..... 37

3.3.1 Validation of the natural frequency evaluation 37

3.3.2 Validation of STL evaluation 39

3.4 Vibro-acoustic investigation 40

3.4.1 Comparison between three different types of sandwich panels 40

3.4.2 Comparison between different boundary conditions: CCCC, CSCS, SSSS ……..47

3.4.3 Comparison between different geometric properties of the honeycomb core ……..51

CHAPTER 4 SOUND RADIATION RESPONSES AND SOUND TRANSMISSIN LOSS CHARACTERISTCS OF A TRUSS CORE SANDWICH PANEL FILLED WITH VARIOUS ABSORPTION MATERIALS..... 56

4.1 Introduction..... 56

4.2 Model establishment and numerical methodology 59

4.3 Validation studies..... 63

4.3.1 Validation of free vibration results with simulation and theory..... 63

4.3.2 Comparison of radiation modes predicted by 3D and 2D finite element models for the panel..... 66

4.3.3 Validation of the STL evaluation 67

4.4 Numerical results and analysis..... 68

4.4.1 Acoustic analysis based on mineral-porous and wood-based porous materials ……..68

4.4.2 Acoustic analysis based on wood-based absorption materials 72

4.4.3 Acoustic analysis based on different material of face sheets 76

CHAPTER 5 CONCLUSION AND DISCUSSION 78

CHAPTER 6 FUTURE WORK 81

CHAPTER 7 BIBLIOGRAPHY 83

CHAPTER 8 STATUS OF PRIMARY PUBLICATION 90

CHAPTER1 INTRODUCTION

1.1 Background

Sandwich panels, with various geometrical cores, have received extensive attention in the aerospace [1], automotive [2] [3], and railway industries [4], as well as in the field of marine [5] engineering. The sandwich panel is typically composed of thin and stiff top and bottom face sheets combined with a thick and relatively less stiff core. The face sheets are used to bear structural loads. The core's function is to provide shear stress transmission between the two face sheets with a lightweight design to achieve remarkable performance in terms of heat dissipation, vibration control and energy absorption [6]. Recently, vibro-acoustic responses and STL characteristics of the honeycomb sandwich panel have been of practical value and this topic has always been of interest to researchers due to their light weight and energy efficiency.

Conventional sandwich structures are typically made of aluminum and offer a superior stiffness to weight ratio as well as an outstanding STL performance at low and middle frequencies [7] [8] but composite sandwich panels have been playing a more important role in recent years as a replacement for conventional metals. The reason behind this change is that composite structures provide dramatic advantages for weight flexibility to meet design requirements, offering a 20%-30% decrease in weight compared to their conventional metal counterparts [9]. Absorption materials are often considered to suppress resonance and improve structural acoustic performance. Sandwich structures filled with glass and mineral-fiber porous media, which are able to enhance structural damping without affecting structural stiffness, have been widely discussed and analyzed

in the literature [10] [11]. However, P. [12] found sandwich structure designs which incorporate acoustic constraints are always denser and larger in size than those which only consider mechanical constraints. Therefore, research has focused on achieving desirable STL performance with a balance of reduced mass, volume and cost.

1.2 Research subjects and contributions

Although many studies have been conducted by researchers and engineers on optimizing the sandwich structures, one of the challenges has been reducing the sandwich structure weight and volume without lowering its acoustic performance. Effective noise control in the low frequency range needs to be addressed in engineering practice but there is little research available in the literature. Hence, the sound radiation problem and STL behavior of composite FRG honeycomb sandwich panels and wood-based-porous-medium-filled truss core sandwich panels are investigated.

The software package, ACTRAN, is employed to derive model solutions and analyze the vibro-acoustic responses of the models due to its ability to solve acoustic problems [13] [14]. The sandwich theory is applied to investigate the free and forced vibrational behavior of the panel, assuming the geometrical core is an orthotropic structural layer. The equivalent orthotropic panel is mathematically modeled by the boundary and shell element method. The methodology used to investigate the sound radiation problems and STL behavior is based on the Rayleigh integral method to integrate the square pressure on a hemisphere in the far field. A comparison is performed between the simulated results and theoretical data to demonstrate the accuracy and reliability of the present

approach. This may provide useful guidance for quantitatively investigating the vibrational and acoustic behaviors and for designing new sandwich panels.

Conventional metal honeycomb sandwich panels are widely used in aeronautical and astronautically fields due to their acoustic performance, whereas, they are very limited in their application to building constructions because of their high density and large occupation of volume. As an alternative to traditional aluminum counterparts, composite fiber reinforced plastic (FRP) honeycomb sandwich panels are well used in practice due to their high strength-weight ratio. However, their poor noise control capability in the low frequency range is its notable disadvantage. The drawbacks are addressed in chapter three by applying FRG composite material to the face sheets of the commonly used honeycomb panels.

The vibro-acoustic behavior of wood-based-porous-medium-filled truss core sandwich panels is discussed in detail. PUF foam-filled truss core sandwich panels are widely used in industry for their ability to improve sound insulation and mitigate resonance. However, its capacity of noise control under low frequency range with low cost and environmental-friendly design is undesirable. The wood-based-porous-medium-filled truss core sandwich panel is investigated to overcome the flaws of PUF foam-filled truss core sandwich panels while keeping their advantages. The results reveal the wood-based-porous-medium-filled truss core sandwich panel, perform better in noise control in the low frequency range with a lower cost and environmental-friendly design while keeping the comparable functions of PUF foam-filled truss core sandwich panels. A wood board-filled truss core with epoxy-carbon face sheet sandwich panel is found to be the optimal design compared to two commonly applied types of truss core sandwich panel because of

its excellent performance with respect to its low frequency noise control and light-weight design.

CHAPTER 2 LITERATURE REVIEW

2.1 Sound insulation concepts

“Noise is unwanted sound from activity in certain rate and time, which can cause human health problems and environmental comfort” [15]. Generally speaking, the variation of the audible sound pressure is from 20μpa to 100pa under standard air pressure of 105Pa. [16]. The theory of sound detection is based on vibration , which is created when the sound pressure strikes surfaces or other sound barriers, when interacting with the human ear [17]. The vibrated surfaces or other sound barriers give rise to the changes in vibrational and normal static pressure, generating sound waves [18]. Sound waves arise from the vibrating object and are propagated from the disturbance in the fluid or solid. The motion of an element drives the nearest particle of air into motion, which establishes a series of compressive and expansive waves because of pressure differences in the transporting medium [19] [20]. The sound, as a function of frequency, is emitted longitudinally. Theoretically, the reason why the longitudinal sound waves occur is because of the difference in air compression and expansion [21]. Two main regions are formed during the sound wave transmission. One represents the zone where the air molecules are crowded together, causing a high pressure zone and another zone with low pressure, resulting in expansion [22]. The difference in air pressure is as a driving force instigating the individual molecule to move side by side, leading to the propagation of the sound speed at which a compression propagates through the medium [23]. Different transmitted media determine the propagation of different sound speeds [24].

The two noise control are passive and active. The active noise control method is based on Yaung's interference principle to artificially attenuate the energy of the original noise [25]. Passive noise control can be achieved by interacting between sound and materials or the transformation of sound energy into other forms, in which the sound can be reduced by vibrational absorption, sound absorption and sound insulation, with damping materials [26].

Sound transmission loss can reflect the ability of the structural sound insulation characteristic itself. Noise attenuation is related to the structural acoustic performance and the impact of sound absorption materials and structure-borne sound transmission paths. Insertion loss represents the measurement results of sound pressure differences with respect to a specific point. The affecting factors come from practical site conditions and the sound pressure differences between the original sound waves and the sound waves passing by the sound barrier structure.

Name	Notation & Definition	Diagraph
Sound Transmission Loss	*TL=10lg(Ii/It)*	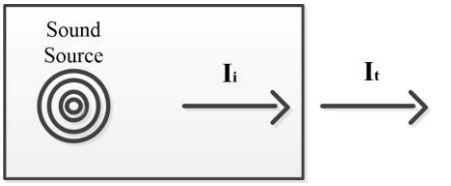 I_i ---incident sound power I_t ---transmitted sound power
Noise Attenuation	*NR=L1-L2*	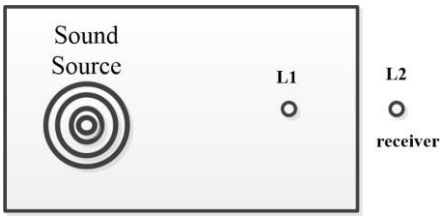 the difference of sound pressure po (L_1 and L_2) with repect to two specifi points P_1 and P_2
Insertion Loss	*IL=L0-L*	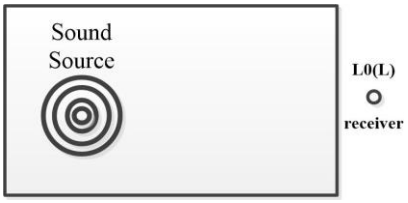 L_0 ---incident sound pressure level L ---transmitted sound pressure level

Fig. 2.1 Three methods for measurement of sound insulation

2.2 Sound insulation formula

The unit for sound intensity is the decibel and it can be measured using a sound-level meter. Sound insulation is defined as the use of noise barriers to reflect or absorb sound wave energy to reduce the sound pressure between a specified sound source and receptor. Using noise barriers to attenuate the noise is the most effective method for road, rail, and industrial noise sources [27]. Factors such as barrier position, layout, shape, material density, and dimensions should be taken into account when designing and constructing barriers.

Incident sound waves are waves striking the noise barriers and being reflected or transmitted. The transmitted sound is measured to determine the acoustic performance of the structure as a noise barrier with respect to the surrounding spaces. The notation, τ is the sound transmission coefficient, which can be expressed as:

$$\tau = \frac{\mathrm{I}_{\text{tranmitted sound power}}}{\mathrm{I}_{\text{incident sound power}}}$$

where τ is a frequency-dependent physical property of the material. The sound absorption coefficient demonstrates the amount of sound energy absorbed by a material and defined as the ratio of absorbed energy to incident energy. A larger sound absorption coefficient implies more of the sound is absorbed and less is reflected back [28].

The sound transmission loss (STL) is the logarithmic ratio of the incident energy to the transmitted energy and is based on the transmission coefficient formula.

$$\mathrm{STL} = 10 \log 1/\tau$$

2.3 The principle of sound insulation

2.3.1 The principle of sound insulation for a single-panel structure

A single panel refers to a one layer wall without any other combination of sandwich layers. Sound insulation performance of a single panel is affected by structural area and the natural frequency properties. Sound transmission loss can be described by separating the sound transmission loss curve (Figure 2.3.1) into three distinct portions: stiffness-controlled, damping-controlled and mass-controlled. The STL associated with the stiff portion is related to the portion of the curve from zero to the first resonant frequency. In this region, the variation between the STL and stiffness is consistent. This is because the structural stiffness increases; the variation of the panel is attenuated, which contributes to a higher sound insulation performance. The STL within the damping-controlled portion depends on the structural internal damping property, which is related to a narrow frequency band close to the resonant frequencies. The sinusoidal pattern reflects the influence of damping properties, and the shift in the resonant frequencies amplifies the magnitude of the damping. The damping-controlled region is regarded as resonant region, where the high amplitude vibration occurs when the external sound frequencies are close to or equal the natural structural frequencies. The reason behind this is because of the high level of displacement resulting in a transfer of large amounts of sound energy [29] [30]. The mass-controlled portion corresponds to the scope after the first resonance frequency. In this region, the STL curve is proportional to the mass, which is known as the “Mass Law”. With increasing mass, more energy is consumed, contributing to higher sound transmission loss behavior [31] [32]. In this region, the normal incidence transmission loss can be approximated by:

$$TL_0 = 10\log[1 + (\frac{\omega\ \rho_s}{2\ \rho\ c})^2]\ \text{dB}$$

where:

ω = sound frequency $\left(\frac{\text{rad}}{\text{sec}}\right)$,

ρc = the characteristic impedance of the medium (415 rayls for air at standard temperature and pressure)

ρ_s = mass of panel per unit surface area

The random incidence transmission loss is:

$$TL \approx TL_0 - 10\log(.23TL_0)\ \text{dB}$$

Sound transmission loss is a function of frequency, which is like the relationship between velocity and time. The sound transmission behavior for a material differs significantly with changing frequencies. In Region III, coincidence between the sound wavelength and structural wavelength further decrease the STL.

The sound transmission loss has a negative value rather than zero as the lowest value, because the simulation is based on the infinite plate model. The incident sound is normalized to the area of the plate, whereas the power can also be transmitted to a wider area by diffraction. Hence, the ratio of the radiated sound and incident power can be greater than unity for the case of the plate trip, which has a finite dimension in one direction [33].

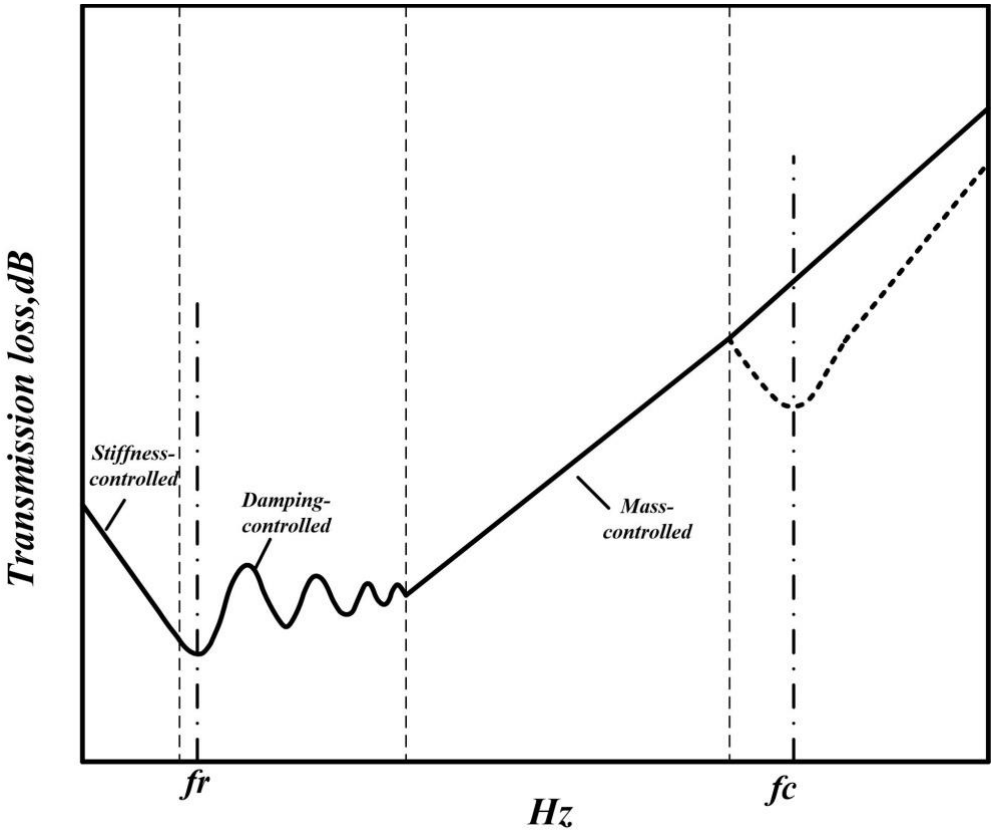

Fig. 2.3.1 Sound transmission loss (dB) curve

2.3.2 The principle of sound insulation for single-panel structures

Based on the mass law, a high sound insulation performance can be achieved by increasing the structural area and mass (enlarging the structural thickness). However, the limitation of a single plate results in poor sound insulation in practice. In construction, the two-panel structure is typically composed of two face sheets and a space in between (Figure 2.3.2). When the incident sound waves strike the wall or other partially absorbing partition between the two spaces, some of the sound waves are reflected(space 1), and the remaining sound waves are transmitted into the adjacent space (space 2). The same sound transmission procedure occurs for the second wall. Except for the energy consumed in the cavity, the incident sound power experiences transmission loss twice when it strikes the panel. The sound power can be decreased significantly this way.

The fundamental principle for sound insulation of two panels is based on the mass law. When the external sound waves strikes the structure, three basic scenarios are going to occur which are because of the relationship between the incident frequencies and incident frequencies : (1) f (incident frequency) $< f_r$ (resonance frequency). The impact of air in the space on sound insulation performance can be ignored, especially where the gap between the two frequencies is wider. The sound transmission is proportional to the area, and equals to the sum of the sound transmission of the two panels respectively: (2) f (incident frequency) = f_0 (resonance frequency). A sharp dip occurs because of high transmission of sound energy. (3) f (incident frequency) $> \sqrt{2}f_0$ (resonance frequency). Sound transmission increases significantly. When the thickness of the cavity is close to an integer multiple of half the wavelength of the incident sound wave, there will be a

series of standing wave resonances between the two walls. The upward trend tends to flatten out compared with the previous high speed growth trend.

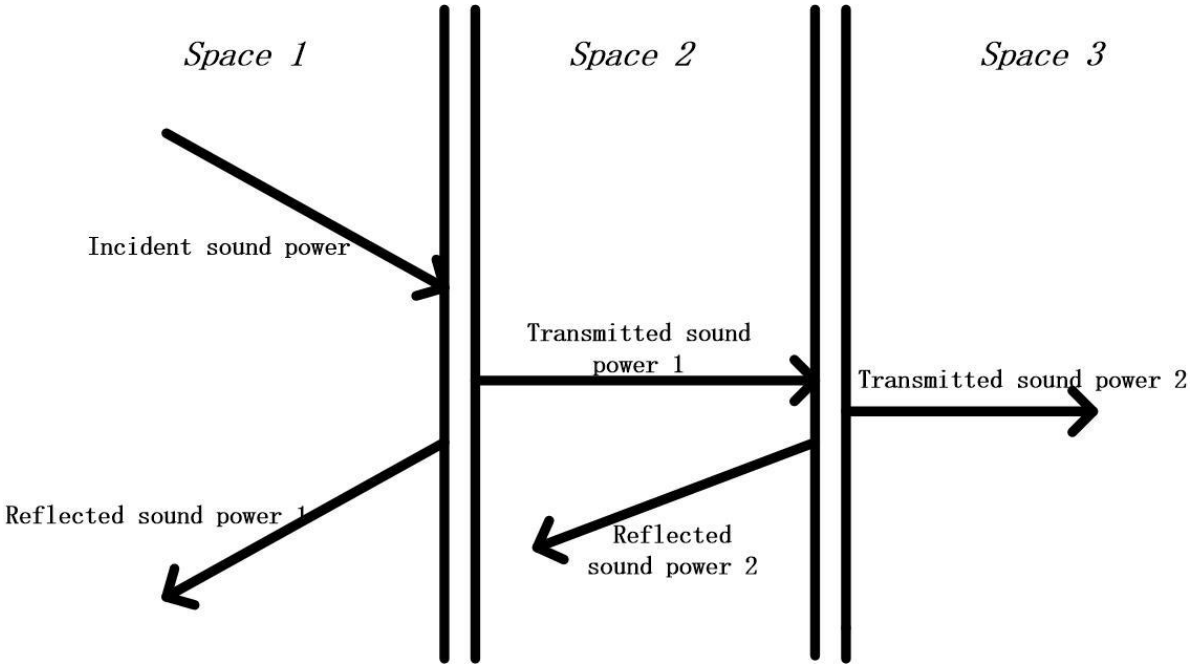

Fig. 2.3.2 Schematic for the sound insulation of two walls

2.3.3 The principle of sound insulation for single-panel structure

The honeycomb core design influences the overall structural resonant frequency. In addition, the deformation and damping of the unit honeycomb core can accelerate energy consumption. The gap between the FRG face sheets and aluminum honeycomb core is wide enough to achieve a desired acoustic performance with a light weight design.

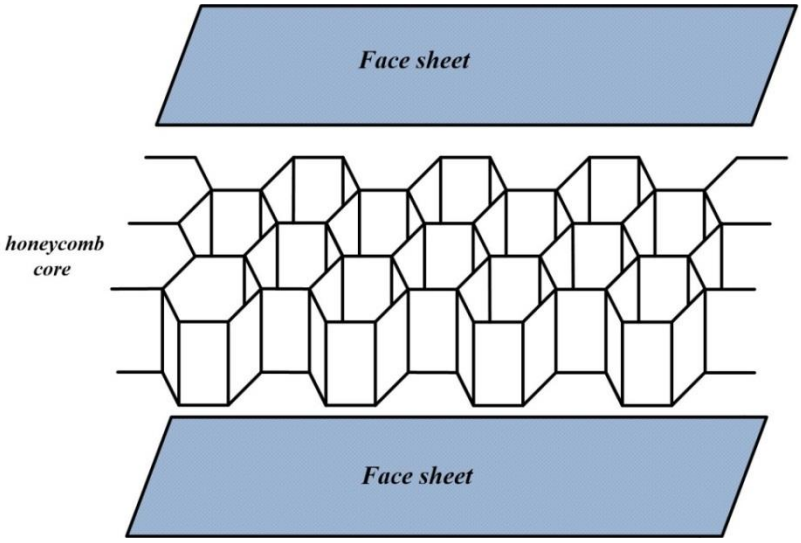

Fig. 2.3.3 Dimension of honeycomb core sandwich panel

CHAPTER 3 VIBRO-ACOUSTIC RESPONSES OF A SANDWICH PANEL WITH ALUMINUM HONEYCOMB CORE AND FABRIC REINFORCED GRAPHITE FACHINGS

3.1 Introduction

A typical honeycomb core sandwich panel is shown in Fig. 2 (a) and (b) [34], with dimensions h, l, m, s, t, a, and b. h is one half of the core height, l is the sidewall length, t is the cell wall thickness, s is the cell size, m is the height of the face sheet, and a and b are the length and width of the honeycomb core sandwich panel, respectively.

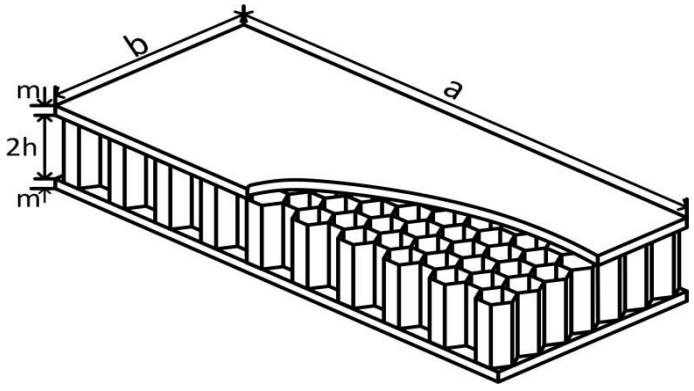

(a) Dimensions of the honeycomb core sandwich panel

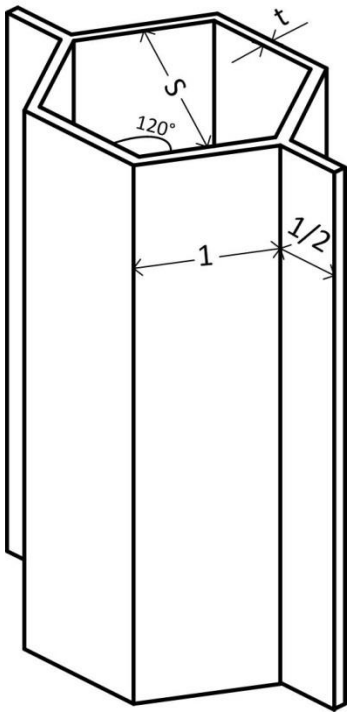

(b) Dimensions of the unit cell honeycomb core

Fig. 3.1 Honeycomb core sandwich panel

Recently, vibro-acoustic responses and STL characteristics of the honeycomb sandwich panel have been of practical value and this topic has always been of interest to the researchers due to the features of manufacturing lightweight and energy efficient panels. The boundary element method [35] is well established as an effective computational way to predict vibro-acoustic problems. It can be derived by recasting the governing partial differential equation as a boundary integral equation, which is made discrete by means of Green's second theorem. A reformulation for Green's second theorem was applied by S. and D. [36] to derive the boundary integral equation and make the boundary element method available for the entire wave number range. The results were compared with the measured sound power to demonstrate the accuracy and reliability of the modified

computational method. The Rayleigh integral method can determine the radiated sound pressure simply and efficiently for a vibro-acoustic problem with an acoustic field exterior to a flat plate set in an infinite co-planar rigid baffle [37] [38]. S. [39] demonstrated a sound insulation structure as a thin structure and mathematically modelled the acoustic barrier by the boundary and shell element method.

The corresponding acoustic studies based on the Rayleigh integral method can be found in the literature. L. & K. [40] studied the STL characteristics of sandwich plates with viscoelastic cores in the diffused sound field with simulation and experimental results, and analyzed the effects of damping on structural acoustic behavior. An acoustic study of an aluminum honeycomb sandwich panel was conducted by M. et. al. [41] to improve its sound insulation capability and optimize the structure by way of varying the honeycomb geometries. M. et. al. [42] numerically investigated the vibro-acoustic responses and STL behaviors of FRP composite honeycomb panels which were mathematically modeled with the shell element method. They demonstrated the advantages of FRP composite honeycomb panels over conventional aluminum honeycomb panels and determined the composite honeycomb panel can be used as an alternative to metal counterparts. Since the effect on sound transmission comes from structural stiffness, damping and mass properties, it is impossible to only investigate acoustic problems based on the unique core of a honeycomb sandwich structure [43]. Therefore, it is of critical significance to predict the STL and explore the effects of a variety of structural geometries and boundary conditions on the structural acoustic behavior. G. et al.[44] investigated the effects of nine combinations of boundary conditions on the average radiation efficiency of rectangular plates. An investigation of

the effects of a variety of geometries, such as face sheets, cell size, and core height on the vibro-acoustic characteristics of the sandwich panel was conducted by A et al. [45].

An equivalent 2D finite element model is commonly used to investigate the vibro-acoustic responses and STL characteristics of honeycomb sandwich panels, which allow for a decrease in the post-processing time [46], sample mesh connectivity and computational cost. The mechanical parameter characterization is of significant importance [47], [48]. Even though the existing equivalent methods all have their own limits due to the fact that they are obtained with different theories [49] are commonly used to simplify the complex honeycomb sandwich structure model and derive the equivalent elastic properties of the honeycomb structure: sandwich plate, equivalent plate, and honeycomb plate theory. The natural frequencies of a honeycomb sandwich panel were studied by X. et al [50] based on three different equivalent theories involving two load cases, and the results among the three equivalent theories was very narrow. I. [18] demonstrated the computational results from the equivalent theories were practically sound in the finite element analysis when compared with the theoretical results. The results based on honeycomb plate theory are most closely aligned with the theoretical results but more computational time is required [51]. J. K. et al [52] studied the strength of aluminum honeycomb sandwich panels from in theoretical and experimental aspects. N. et al [52] put forward an improved method based on the existing equivalent theories and applied it to a mechanical investigation of fiber-reinforced plastic honeycomb sandwich panels.

One of the challenges faced by the researchers and engineers is reducing the weight and space of the sandwich structure without lowering its acoustic performance. An effective

noise control in the low and middle frequency ranges is a problem that needs to be addressed in engineering practice and research can rarely be found in the literature. The vibro-acoustic problem and STL behavior of FRG honeycomb sandwich panels is investigated with the employment of ACTRAN, which is used to derive the model solution and analyze the acoustic performance of the models. Furthermore, the ACTRAN functions mentioned previously have been widely used by engineers and researchers [13] [14] because of their ability to simulate acoustic problems.

Conventional aluminum honeycomb sandwich panels are widely applied in aeronautical and astronautically fields due to their acoustic performance but they are very limited in their application to building construction because of their high density and large volume. FRP honeycomb sandwich panels are well accepted as an alternative to their traditional aluminum counterparts due to their high strength-weight ratio. However, its drawback is its poor noise control capability in the low frequency range. It is anticipated the drawbacks will be overcome with a sandwich panel, honeycomb structure, and FRG face sheets. The sandwich theory is applied in the simulation to investigate the panel's free and forced vibration behavior, assuming the honeycomb core is an orthotropic structural layer. The equivalent orthotropic panel is mathematically modeled with the boundary and shell element method. The methodology is applied to investigate the vibro-acoustic and STL problem and it is based on the aforementioned Rayleigh integral method to integrate the squared pressure on a hemisphere in the far field. A comparison between the simulated results and experimental data demonstrates the accuracy and reliability of the present approach. This may provide useful guidance for quantitatively investigating the vibrational and acoustic behaviors, and designing new sandwich panels.

3.2 Model establishment and numerical methodology

The composite honeycomb sandwich panel STL is investigated by analyzing its free and forced vibration response, and the STL characteristics are presented.

(1). The sandwich theory:

The sandwich theory equalizes the honeycomb sandwich core as a continuous, homogeneous, and orthotropic layer. The equivalent theory only simplifies the honeycomb core by assuming the core can resist transverse shear deformation and possess in-plane stiffness, while the top and bottom face sheets satisfy the Kirchhoff hypothesis.

The Kirchhoff hypothesis is satisfied with the following assumptions:

- The plate thickness is small compared with the leading dimensions but it cannot be ignored with respect to the lateral deflection which becomes comparable to the circular angle.
- The effects of three-dimensional stress can be ignored
- The plate is symmetric in fabrication about the mid-surface
- The transverse loads applied to the plate can be distributed over the full surface areas
- The support conditions do not create a significant extension of the mid-surface.

$$E_x = E_y = \frac{4}{\sqrt{3}}\left(\frac{t}{l}\right)^3 E_s \qquad G_{xy} = \frac{\sqrt{3}\gamma}{2}\left(\frac{t}{l}\right)^3 E_S$$

$$G_{xz} = \frac{\gamma}{\sqrt{3}}\frac{t}{l}G_S$$

$$\upsilon = \frac{1}{3} \tag{1}$$

where E_x, E_y and G_{xy}, G_{xz}, G_{yz} are the equivalent Young's moduli and shear moduli, respectively. E_s, G_s are the engineering constants of the core; ν is Poisson's ratio, t is the cell wall thickness, l is the sidewall length, and γ is the corrected coefficient with a value between 0.4-0.6 [51]. Modeling the middle honeycomb core as an equivalent orthotropic approximation reduces the pre- and post-processing time to calculate the vibrational response.

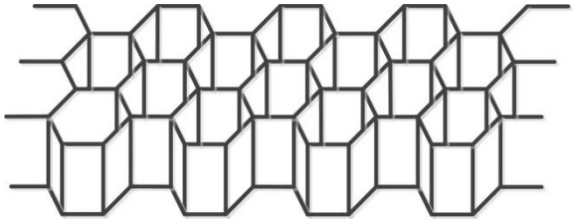

Fig. 3.2 a Honeycomb core

Fig. 3.2 b Equivalent orthotropic layer

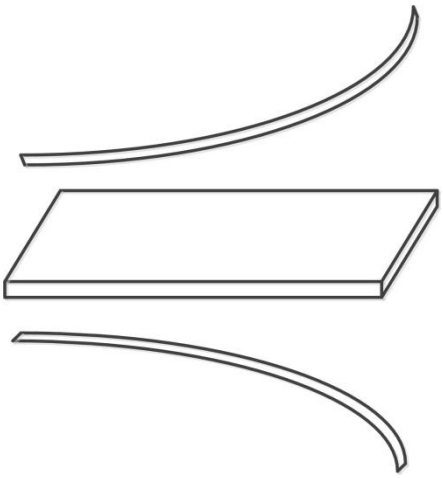

Fig. 3.2 c Attaching two face sheets in Actran

(2) Based on the equivalent theory, the middle layer is extracted, and the corresponding geometric model is created in Ansys. The Hypermesh is applied to analyze the 3D finite elements of the viscoelastic shells. The meshed finite element model is imported into Actran to investigate the acoustic performance. The 3D finite elements for the viscoelastic shells (Fig. 3 b) are applied to represent the honeycomb core (Fig. 3 a), which features a unique proprietary formulation ensuring no thickness-locking and no shear-locking effects occur. The following form shows the supported topologies in 3D elements:

Table 3.2 Supported topologies in Actran

3D Elements	
HEX08	Yes
HEX20	Yes
PEN06	Yes
PEN15	Yes
TET04	No
TET10	No
PYR05	No
PYR13	No

Each node supports three degrees of freedom, the displacement components u_x, u_y and u_z of the node along the x, y and z directions.

An orthotropic solid material is characterized by ten parameters, which are : the three Young's moduli, E_1, E_2 and E_3, three Poisson's ratios, v_{12}, v_{13} and v_{23}, three shear moduli, G_{12}, G_{13} and G_{23}, and the solid density ρ_s.

The two GPR face sheets are created and attached to the equivalent orthotropic layers as two thin plates as shown in Fig. 4 c (finite elements for viscoelastic thin shells) using a simplified 2D representation,. The finite elements for the viscoelastic thin shells represent three degrees of freedom: the displacement components u_x and u_y of the node along the x and y directions, and the rotation component θ_z of the node along the z axis.

(3) The eigenvalue equation is solved to compute the natural frequency and the mode shape under the clamped boundary condition. The mathematical expression when clamped along the edge's boundary condition is:

$$\left[K - \omega_k^2 M\right]\{\varphi_k\} = 0 \qquad (2)$$

where K is the structural stiffness matrix, M is the structural mass matrix, ω_k is the circular natural frequency of the sandwich panel, and $\varphi_k$is the corresponding mode shape.

(4). A harmonic force of 1 N is applied as an excitation point to find the forced vibration response, and the damping ratio of 0.01 is used for all modes. The forced vibration response is expressed as:

$$M\ddot{U} + C\dot{U} + KU = F(t) \tag{3}$$

where C is the damping matrix, F(t) is the time-harmonic load vector, and $\ddot{U}, \dot{U}$ and U are the acceleration, velocity and displacement vectors of the panel, respectively.

(5) The finite element method is applied in Actran to address the radiated sound power and the diffuse incident pressure field. The acoustic radiation problem, based on the theory of Rayleigh boundary elements (Fig. 4), can be formulated for every element with reference to a vibrating structure whose radiation surface Γ is located in the plane of a rigid baffle:

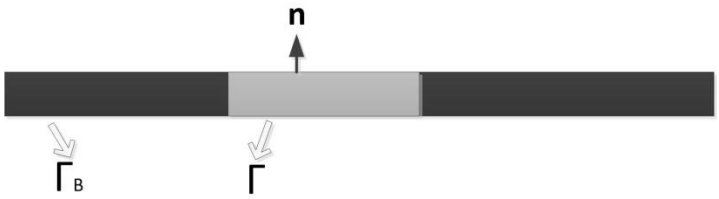

Fig. 3.2 d Plane structure mounted in a plane rigid baffle

$$\Delta p\left(\vec{r}\right)+k^2 p\left(\vec{r}\right)=0 \tag{4}$$

where p is the acoustic pressure, k is the wavenumber, and $\vec{r}$ represents a point with coordinates (x,y,z). This equation must be supplemented with the following boundary conditions:

$$\frac{\partial p}{\partial n}=\rho\omega^2 u_n \quad \text{on T} \tag{5}$$

and

$$\frac{\partial p}{\partial n}=0 \quad \text{on TB} \tag{6}$$

where n denotes the inward normal direction, u_n is the related displacement component, and Γ_B denotes the boundary surface of the baffle.

(6) The sound power radiating from the vibrating panel can be calculated using the following relation:

$$\overline{W}=\frac{1}{2}\mathrm{Re}\left(\oint p(r)\dot{w}^*(r)ds\right) \tag{7}$$

where $\overline{W}$ refers to the sound power, and $\dot{w}^*$ refers to the complex conjugate of the acoustic particle velocity.

(7) In Actran, the diffuse incident pressure field indicates the sound field in which the time average of the mean-square sound pressure is the same everywhere and the flow of acoustic energy in all directions is equally probable.

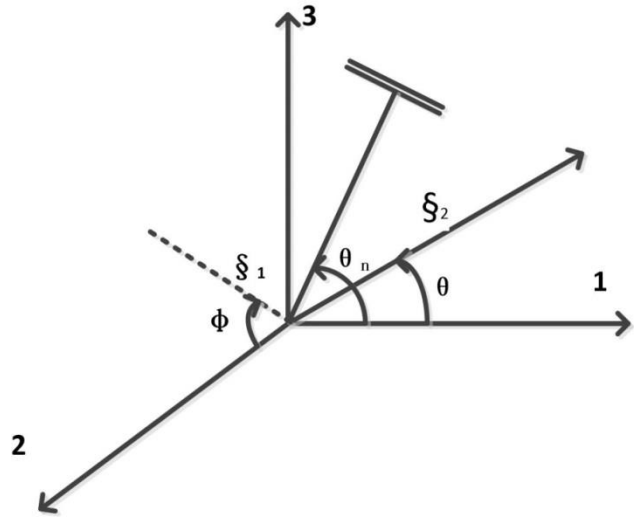

:

Fig. 3.2 e The coordinate system and a particular plane wave.

According to Fig. 5, p_n represents the pressure field related to a particular plane wave (index n), and it can be denoted as $p_n(r,t)$, where $r(r,\theta,\varphi)$ is the vector position of the evaluation point, and t is the time.

The final objective is the evaluation of the spatial correlation function and two points are considered along axis 1: the first point (labeled ζ_1) is located at the origin, while the second point (labeled ζ_2) is located at coordinates (r, 0, 0). If $x_n(t)$ denotes the instantaneous pressure value at the origin for the plane wave, then:

$$x_n(t) = p_n(0,t) \tag{8}$$

The pressure at location r along axis 1 is obtained by converting the spatial interval into an equivalent time interval:

$$p_n(0,t) = p_n\left(0, t-\frac{r}{c}\cos\ \theta_n\right) = x_n\left(t-\frac{r}{c}\cos\ \theta_n\right) \tag{9}$$

The diffuse field pressure along axis 1 is represented by summing an infinite number of plane waves arriving from all directions:

$$p(r,t) = \lim_{N\to\infty} \frac{1}{\sqrt{N}} \sum_{n=1}^{N} p_n(r,t) \tag{10}$$

Substitution of Eq. (10) into Eq. (9) obtains the following:

$$p(r,t) = \lim_{N\to\infty} \frac{1}{\sqrt{N}} \sum_{n=1}^{N} x_n\left(t - \frac{r}{c}\cos\ \theta_n\right) \tag{11}$$

The incident diffuse sound power can be calculated with the relationship between the sound pressure and sound power.

(8) The result obtained from equation (11) is used as input to calculate the corresponding incident sound power:

$$W_i = \frac{\rho_i^2 \cos\theta ab}{2\rho c} \tag{12}$$

where ρ_i is the incident pressure, θ is the incidence angle (rad), and a and b denote the length and breadth of the plate, respectively. ρ is the density of the air and c is the speed of sound.

(8) The expected radiated sound power and incident sound power can be calculated through equations (7) and (12) using the finite element method. The STL, in terms of decibels, is described as:

$$TL = 10\log_{10}\left(\frac{1}{\tau}\right) \tag{13}$$

$$\tau = \frac{Transmitted \quad power}{Incident \quad power} \tag{14}$$

3.3 Validation studies

3.3.1 Validation of the natural frequency evaluation

A study for modes calculation of the sandwich panel conducted by L. et al. [29] is considered to validate the proposed method for predicting the vibration response. The honeycomb sandwich plate area dimensions are 4 m*2 m and the surface layer and core thicknesses are 0.3 mm and 14.4 mm, respectively. The hexagon cell length is 4 mm and its thickness is 0.04 mm. It is tested for comparison and its elastic modulus is 68 GPa, its Poisson ratio is 0.3. The mass density for the two face sheets and the honeycomb core are 2700 kg/m^3 and 40kg/m^3, respectively. The honeycomb sandwich panel's natural frequency is calculated and found to be in good agreement with the results obtained by Hao et al., which can be seen in Table 2.

Table 3.3.1 Natural frequency validation

Modal steps\ Methods	Proposed solution	Academic solution
1	16.6563626678	16.17
2	28.6720412073	25.87
3	46.7510636503	42.14
4	51.7319919889	55.07
5	62.5430999513	64.63
6	66.5000131091	64.45

3.3.2 Validation of STL evaluation

Date from C & K [17] is compared to the results to validate the proposed method for predicting the STL. L & K analyzed a sandwich panel of size 0.303 m*0.203 m with a top and bottom face sheet thickness of 0.5 mm and core thickness of 2 mm. The face sheet and core material densities are 2720 kg/m^3 and 1.60 kg/m^3, respectively. The Young's modulus and shear modulus of the face sheet and core material are 73.2 GPa and 4.12 GPa, respectively. Poisson's ratio of the face sheet and core material is given as 0.33 and 0.4, respectively. The predicted sound transmission loss according to the proposed method agrees with the experimental and analytical data, as seen in Fig. 6.

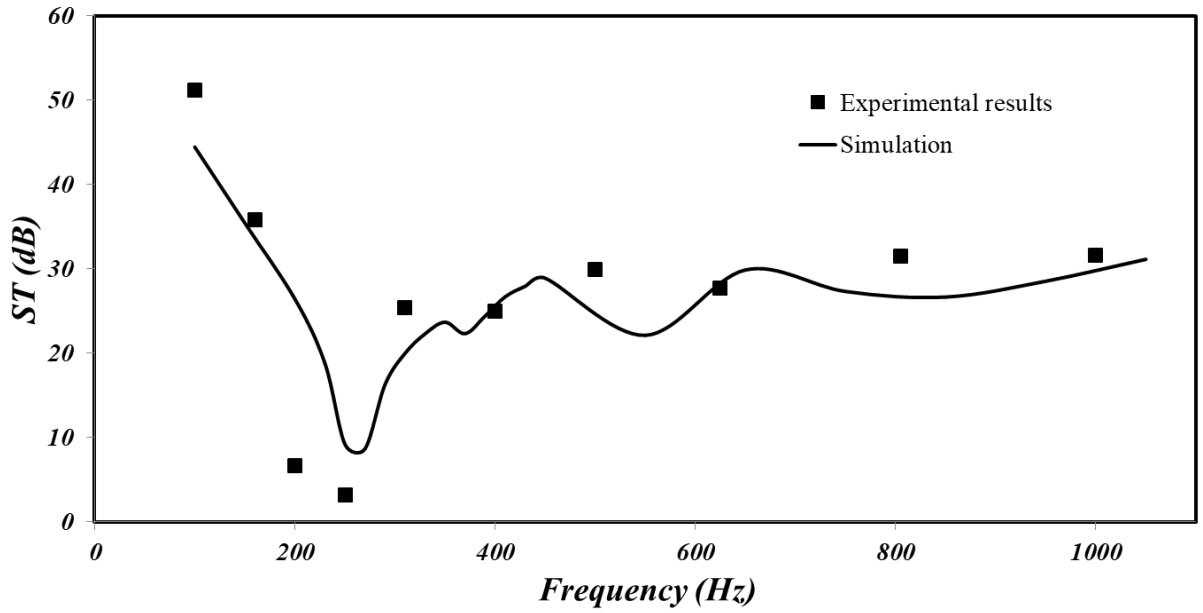

Fig. 3.3.2 Sound transmission loss validation

3.4 Vibro-acoustic investigation

A comparison of the vibration responses and acoustic properties among three types of honeycomb structures is investigated. The effects of various boundary conditions and geometric properties on a FRG honeycomb sandwich structure's acoustic performance are considered. A structural damping ratio of 0.1 is applied for all cases and the target frequency range is 0 to 1000Hz.

Sharp dips always appear in the natural frequencies within the target excitation frequency range, due to elevated sound pressure transmission. The face sheet's height and honeycomb core and the thickness and length of the unit cell have significant effects on the structure's natural frequencies correlated to the modal stiffness and mass factors. The target excitation frequency range used for acoustic analysis is focused on low frequencies, which can be challenging for acoustic engineers. Thus, improving sound insulation of natural frequencies is one criteria in the acoustic analysis. The panel dimensions may be determined based on the aforementioned reasons,.

The tested honeycomb sandwich panel size is $1.5\ \text{m} \times 1\ \text{m}$. The thickness and length of the honeycomb cells is 0.04 mm and 4 mm, respectively. The mechanical properties of the aluminum honeycomb core sandwich panel with plane FRG face sheets are shown in Table (1).

3.4.1 Comparison between three different types of sandwich panels

(1) Aluminum honeycomb core with aluminum panels;

(2) Aluminum honeycomb core with FRP panels;

(3) Aluminum honeycomb core with FRG panels.

The boundary condition for the acoustic performance investigation is clamped edges (CCCC). The mechanical properties are shown in Table 2 [15].

Table 3.4.1 a Mechanical properties of the FRG

Property		
	FRG	Aluminum
Density (kgm^{-3})	1600	40
Young's modulus E_t(GPa)	49	68
Poisson's ratio	0.15	0.3

The natural frequencies of the FRG honeycomb sandwich panel, traditional aluminum honeycomb panel, and FRP honeycomb plates are compared. The FRG honeycomb sandwich structure possesses five radiation models in the targeted frequency range (0-1000 Hz), while there are nine radiation models in the aluminum sandwich plates, and seven radiation models in the FRP honeycomb panel. The excitation point of the forced vibrations response (Fig. 7) should not be a vibration nodal point for any mode within the tested excitation frequency range. Based on this premise, the average RMS velocity responses under the CCCC boundary condition are given in Fig. 7. The RMS velocity response resonance amplitude is highest for the FRP honeycomb sandwich panel, with a value of $8.47e^{-6}$, when compared with the other two cases, which is attributed to its lower density and stiffness. The FRP honeycomb sandwich panel sound power level response (Fig. 8) is the highest among the other two cases, while the traditional aluminum honeycomb plates have the lowest sound power level response. The shift in the natural frequencies will also be high if the material is very stiff. This fundamental theory is reflective of the relatively stable trend for the FRG honeycomb sandwich panel in Fig. 8, due to its higher stiffness property and lower radiation modes. The trend for the STL curve shown in Fig. 9 shows the opposite form compared with its corresponding sound power level curve, which means the sound power level has its peak value at the resonant frequencies, whereas the STL curve has sharp dips in the resonant frequencies because of the high sound power transmission. A random diffuse field with 10 samples are set up in Actran for acoustic analysis to investigate the acoustic behavior for the three types of honeycomb sandwich panels. Based on the convergence study, the layered structural shell element with a mesh size of 63×94 is used in the 1/4 symmetry model. According to Fig.

9, a 14.33 percentage increase in STL is achieved with the FRG honeycomb panel when compared with the FRP honeycomb sandwich panel. Even though the acoustic performance of the FRG is not as good as the conventional aluminum structure, since it has a lower density in accordance with the mass law in the STL curve, a comparable sound effect can still be achieved with a lightweight design. A relatively stable trend appears in the FRG sandwich panel STLs as a result of the relatively higher stiffness properties and lower resonance modes for the three types of honeycomb structures.

Table 3.4.1 b Natural frequency of the three honeycomb structures

Mode step	Natural Frequency		
	Aluminum	FRP	FRG
1	388.877217786	317.983994345	408.202488862
2	422.683 444533	539.214480718	535.82122545
3	609.377578811	598.809326917	652.526832096
4	723.821052235	709.419612707	917.82824964
5	765.715101851	905.165093682	971.193344669
6	834.317637568	927.366151501	1005.12400845
7	923.690802762	978.134434706	1013.28951556
8	929.16102066	1064.16974213	1058.50986895
9	932.907576334	1075.49075183	1183.57342158
10	1054.64846616	1185.51468	1196.48127709

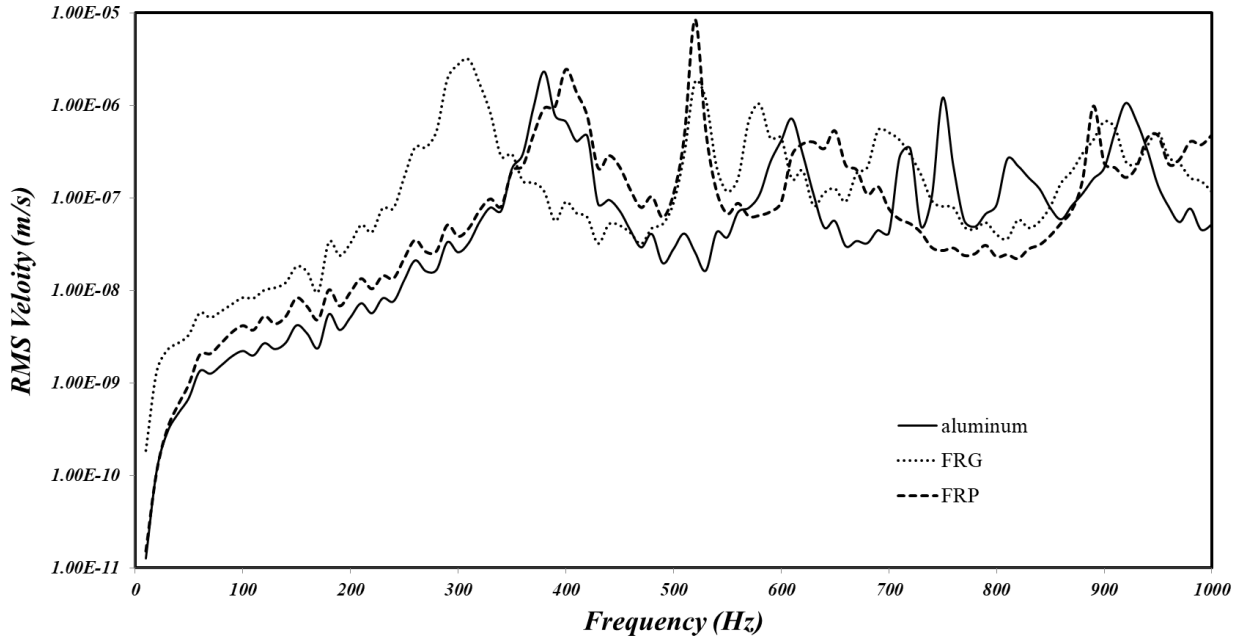

Fig. 3.4.1 a Vibration response of the three honeycomb structures

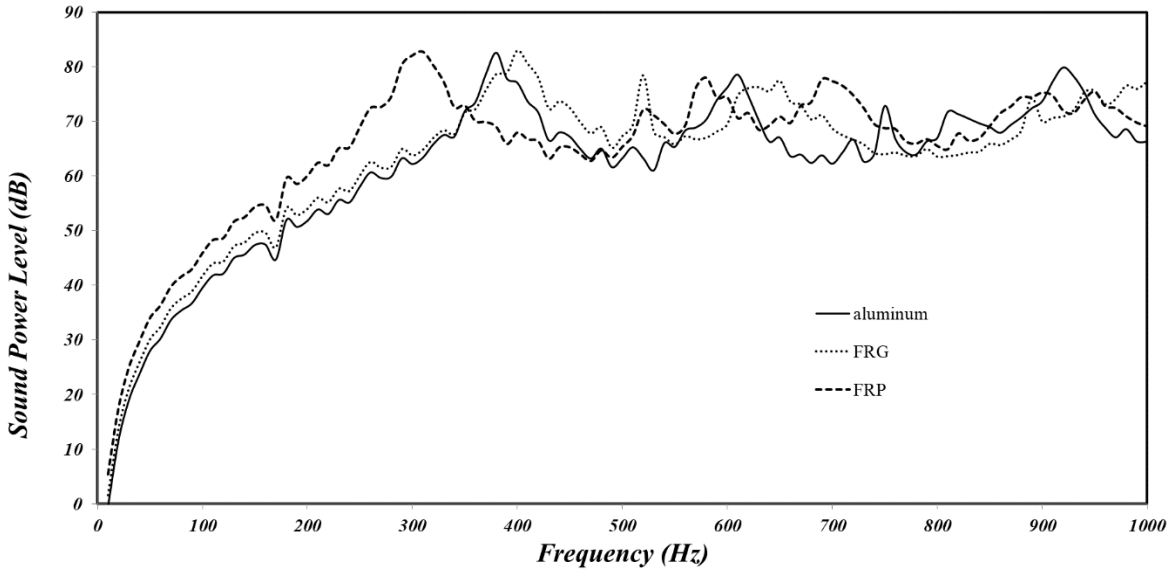

Fig. 3.4.1 b Sound power level of the three honeycomb structures

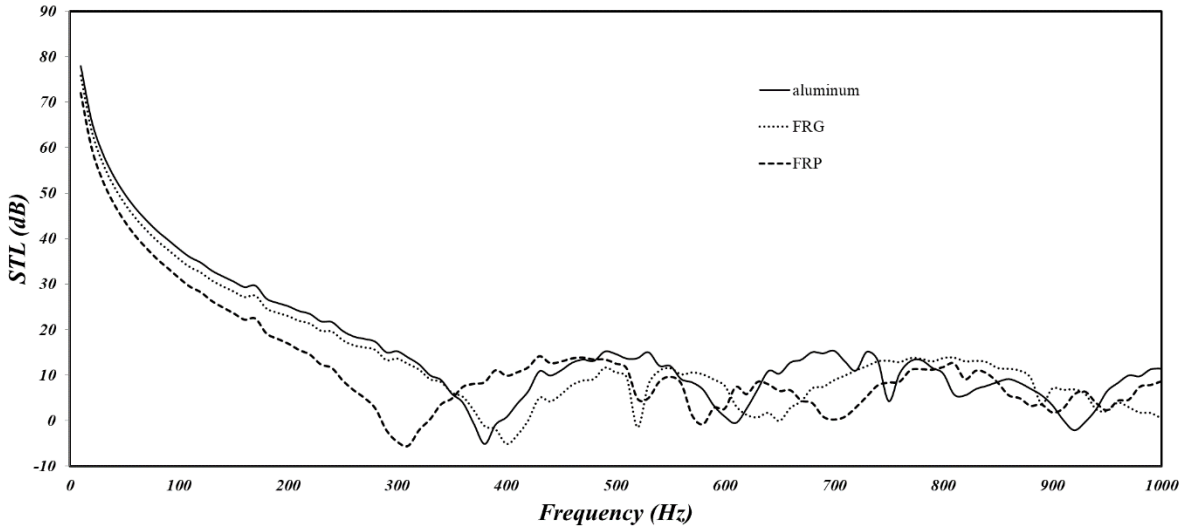

Fig. 3.4.1 c Sound transmission loss of the three honeycomb structures

3.4.2 Comparison between different boundary conditions: CCCC, CSCS, SSSS

In this section, the effect of a variety of structural boundary conditions on the vibro-acoustic response and the STL for the RPG sandwich panel is studied to investigate the influence of stiffness on the target range of excitation frequencies. The boundary conditions include CCCC, SSSS, and CSCS, where C refers to clamped and S refers to supported. The mathematical equation for clamped edges along the x axis is described as $x=0, \omega=0, \partial\omega/\partial y=0$. The CCCC denotes four edges that satisfy clamped edges, CSCS denotes two adjacent sides meeting the clamped criteria and SSSS allows four sides free to move. The natural frequency associated with the CCCC boundary condition is higher than the other two types of boundary conditions. There are nine radiation modes appearing in the SSSS boundary condition, while five radiation modes exist in the CCCC boundary condition. The effects of the different types of boundary conditions on the forced vibration response are shown in Fig. 10. The RMS velocity response resonance amplitude of the FRP honeycomb sandwich panel under the SSSS boundary condition reaches the largest value due to a relatively low density and stiffness. The effect of the radiation modes should be considered with respect to the sound power level response shown in Fig. 11. The number of radiation modes under the CCCC boundary condition is less than under the other two conditions, which means a more stable sound power level trend would appear because of higher sound power transmission. The shift in resonant frequencies under the CSCS boundary condition is the highest because of its higher stiffness. The stiffness in Fig. 12 can be clearly seen within the frequency range before the first natural frequency as well as in the mass-control region. A wider shift appears during each resonance frequency due to the increasing stiffness from the CCCC condition,

which contributes to a more stable trend in the STL. A smaller dip can appear in the STL curve due to a smaller presence of radiation modes, leading to an improved acoustic performance.

Table 3.4.2 Natural frequency of the three boundary conditions

Mode step	Natural frequency		
	CCCC	CSCS	SSSS
1	408.202488862	338.196066395	53.6964298822
2	535.82122545	462.381958045	198.067684778
3	652.526832096	629.049580949	216.624864432
4	917.82824964	719.946049579	367.914060486
5	971.193344669	769.087506355	399.196523752
6	1005.12400845	953.07122048	424.346398629
7	1013.28951556	1010.86785759	516.894247047
8	1058.50986895	1058.50930759	566.797874652
9	1196.48127709	1183.57241641	605.645758994

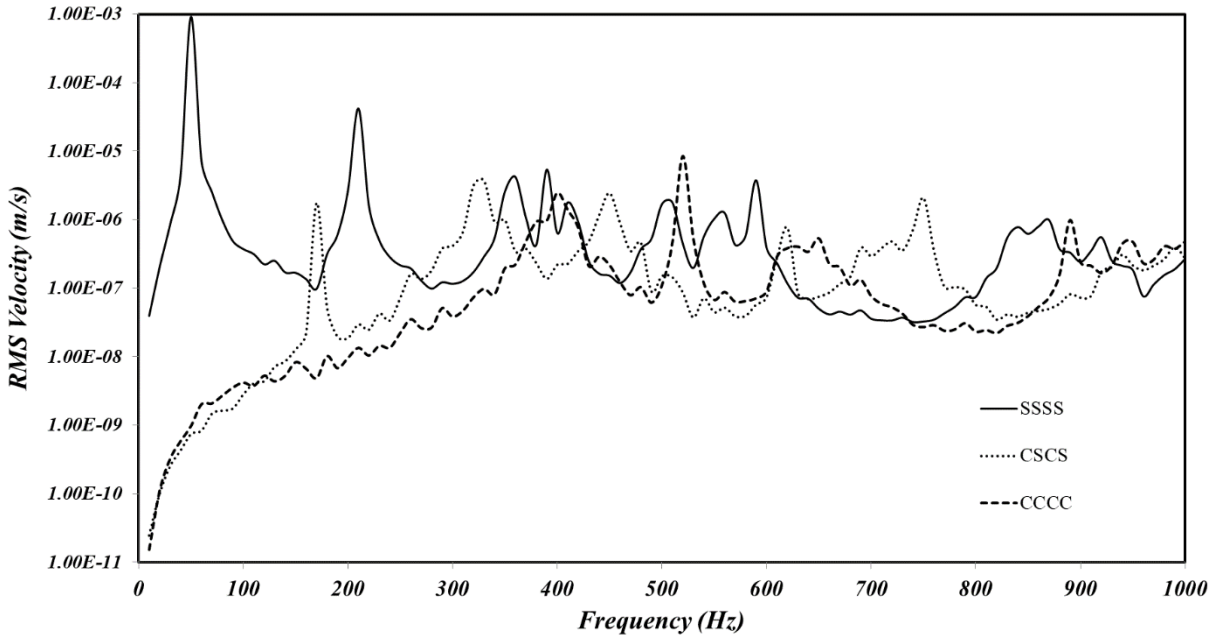

Fig. 3.4.2 a Vibration response of the boundary conditions

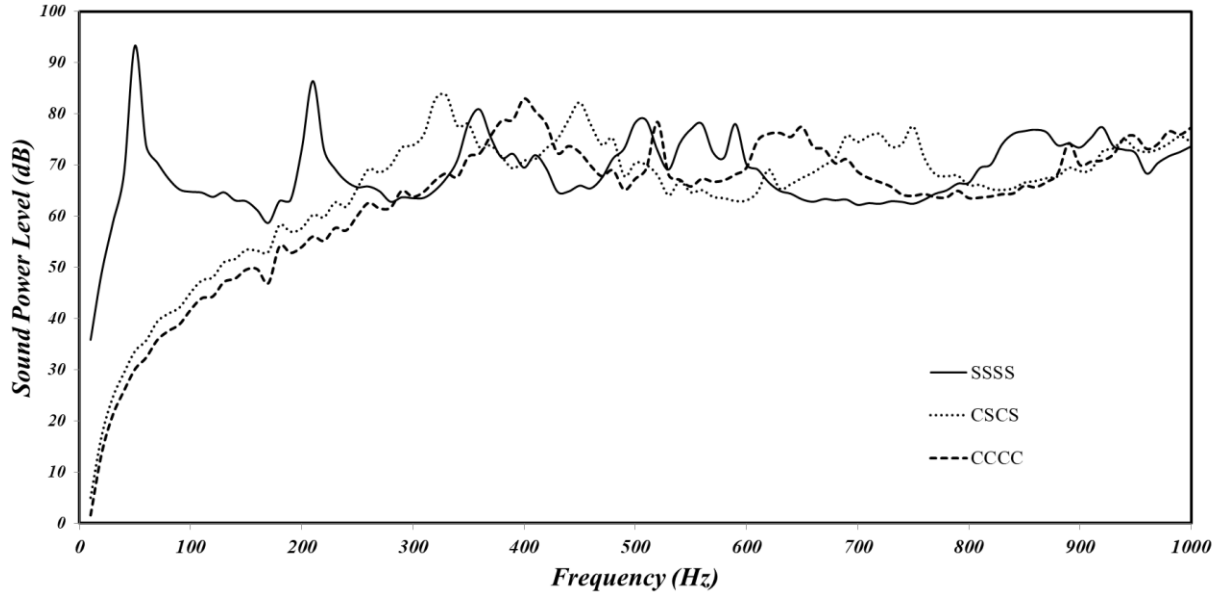

Fig. 3.4.2 b Sound power level of the three boundary conditions

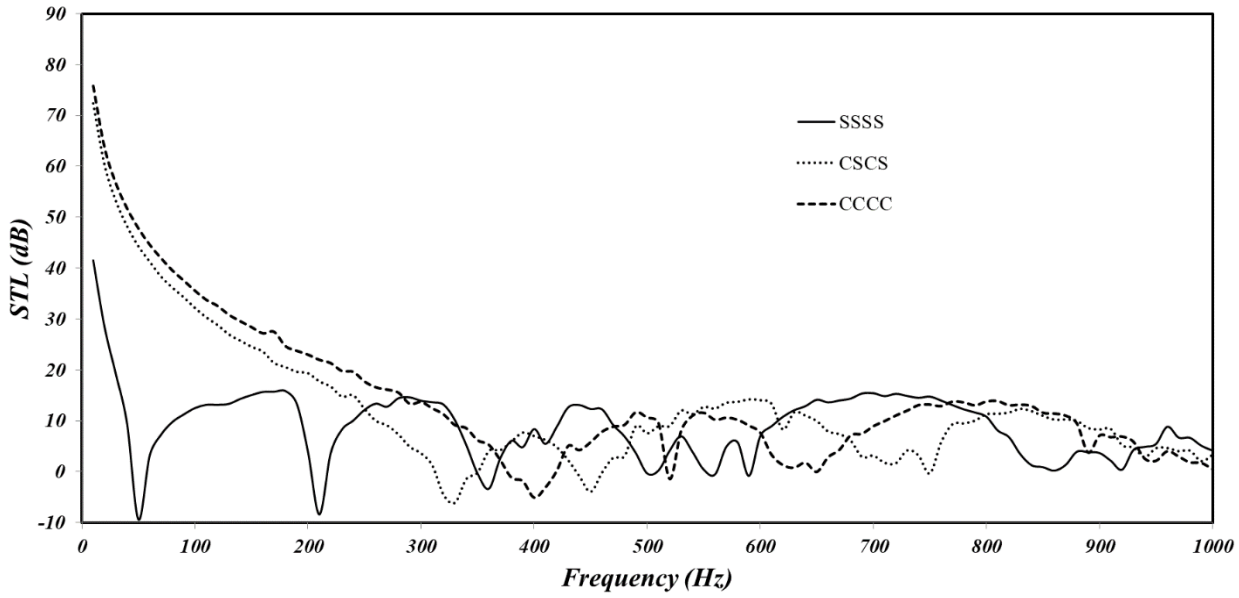

Fig. 3.4.2 c Sound transmission loss of the three boundary conditions

3.4.3 Comparison between different geometric properties of the honeycomb core

3.4.3.1 Effect of cell size

Changes in ell size are related to variations in the cell thickness and size. As a result, the effect of cell size on the honeycomb sandwich panel radiated sound power level and STL, under the CCCC boundary condition is investigated by varying the cell size ratio to 0.046, 0.031, and 0.023. The cell size ratio in the research is the cell thickness to cell length. Fig. 13 (a) and Fig. 13 (b) show the influence of cell size on the honeycomb sandwich panel radiated sound power level and STL under a diffuse incident pressure field. There are no distinguishing differences appearing with the changes in the cell size, which means the radiated sound power and transmission loss are not sensitive to changes in cell size. The reason is the counterbalance between mass and stiffness. The sound transmission

loss in the damping-controlled region is proportionally similar since the damping ratio is assumed to be 0.01 for all cases.

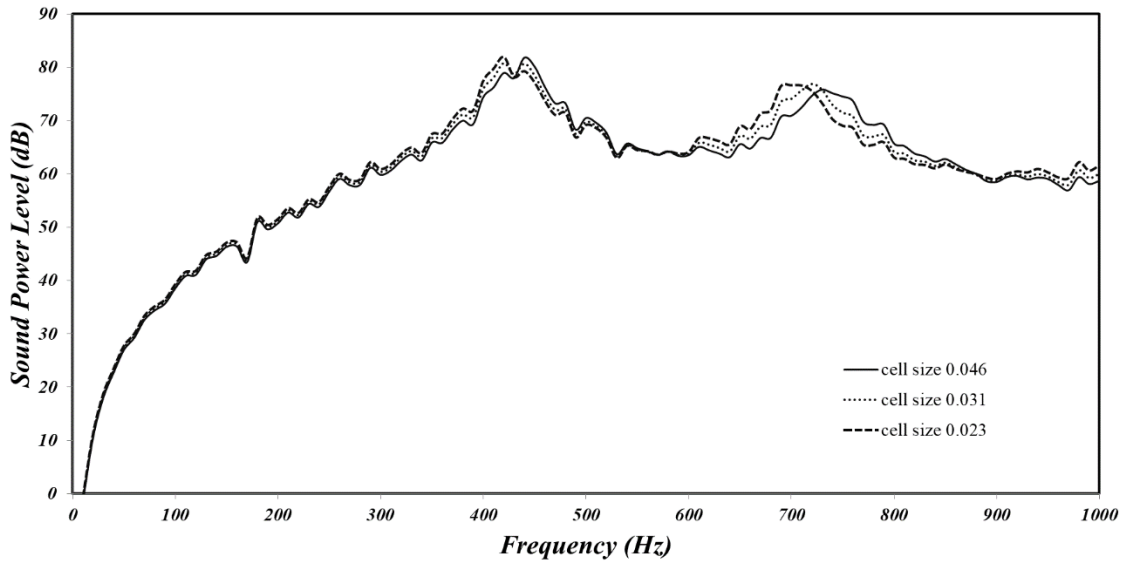

Fig. 3.4.3.1 (a) Sound power levels under different cell sizes

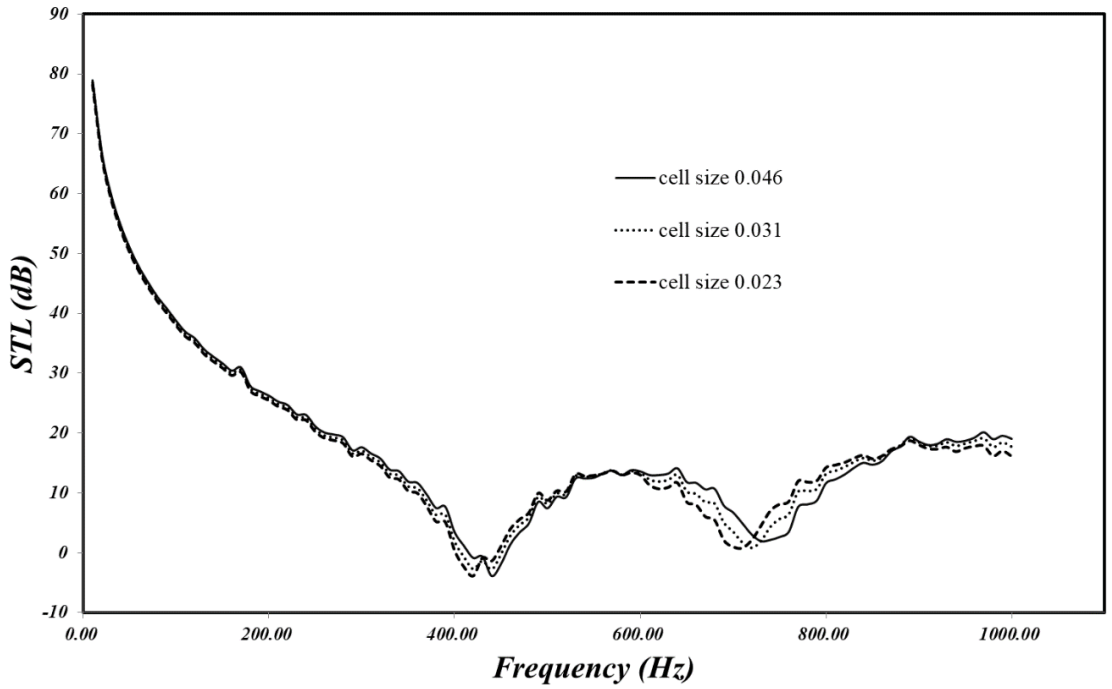

Fig. 3.4.3.1 (b) STL under different cell sizes

3.4.3.2 Effect of the core height

Reducing the panel size is considered due to the space constraints and to achieve a desirable acoustic performance. The tested core heights are 10 mm, 15 mm, and 20 mm, and the corresponding increasing order for the face sheet thicknesses of 2 mm, 1.5 mm, and 0.5 mm are selected. Fig. 14 (a) and Fig. 14 (b) show the effect of the honeycomb sandwich panel core height on the sound power level and STL. the resonant sound power amplitudes in Fig. 15 (a) are significantly influenced by the core height. The changes in STL appearing in the stiffness-domain region in Fig. 15 (b) cannot be clearly distinguished because the variation in core height cannot significantly influence the structural stiffness because of the counterbalancing effect of the face sheet thickness and core height. However, anti-peak curves shown in the mass-domain region are clear, implying the effect arising from the face sheet thickness is more significant than the stiffness. This effect obeys the mass law in the STL curve. The mass-controlled portion corresponds to the scope after the first resonant frequency in the STL curve. In this region, the STL is proportional to the mass. The effect of damping can clearly be seen in the resonant frequencies through the multiple peaks and valleys. A higher STL performance is achieved in the mass-controlled region with a smaller structure.

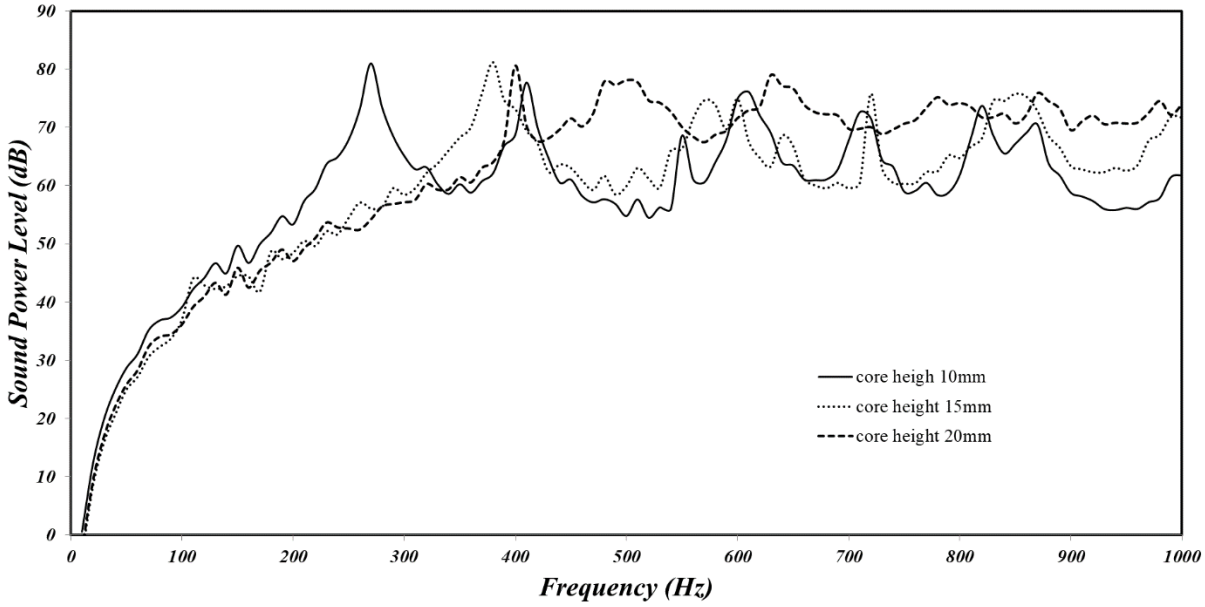

Fig. 3.4.3.2 (a) Sound power level

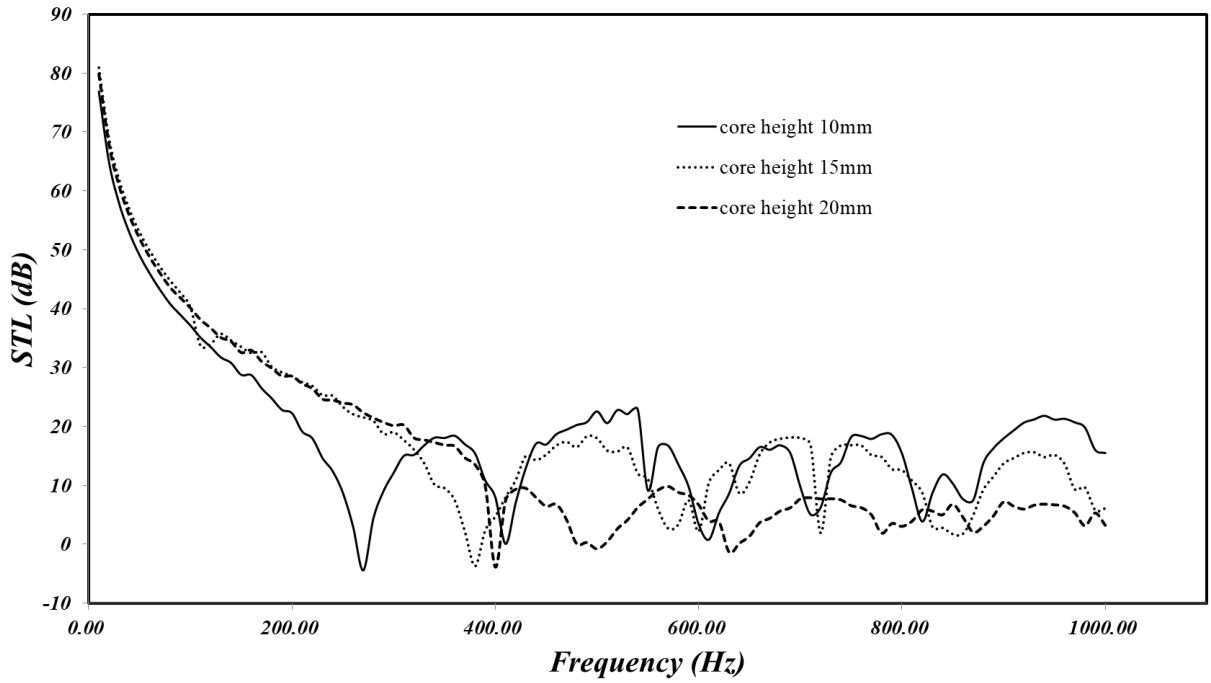

Fig. 3.4.3.2.3 (b) Sound transmission loss, dB

CHAPTER 4 SOUND RADIATION RESPONSES AND SOUND TRANSMISSIN LOSS CHARACTERISTCS OF A TRUSS CORE SANDWICH PANEL FILLED WITH VARIOUS ABSORPTION MATERIALS

4.1 Introduction

Sound absorption material is definitely considered a material that can transmit as much as sound waves [53]. High sound transmission through absorbing materials can be achieved by absorbing as much sound over the same amount of time while reflecting as little as possible. There are multiple factors affecting the capability of absorbing materials. In this chapter, face sheet density, porosity, properties of absorption materials, and hard and soft absorbing materials are discussed.

Density is demonstrated as mass per unit volume and influences the capacity of the absorption materials based on the following formula[54]:

$$Z = \rho cs\frac{A+B}{A-B} \quad (1)$$

Where ρ denotes the density of a material, c is the speed of sound, s represents the cross sectional area, and A+B and A-B are the maximum and minimum wave patterns, respectively. The principle of density to influence the acoustic performance is based on the structural impedance property of the absorbing material and determines the material's ability to reflect sound.

Two kinds of absorption material, bare polyurethane and polyurethane with rice husk, were compared by S. M. A. A. Zaidi et al. [54]. They concluded that a better absorption performance at frequencies ranging between 200 and 1000Hz can be achieved with the polyurethane added to the rice husk, which is due to its higher density. However, absorption is decreased significantly at higher frequencies (around 2000Hz) because that material's overall thickness plays a dominant factor in the high frequency range. The coincidence dip phenomenon at high frequencies was studied by F. Shahani et al [55] and M. I. A. Abdalla [56]. Critical frequency, demonstrated as the frequency in which the incident sound wave is in phase with the reflected wave, leads to the occurrence of coincidence dips and decreases a material's ability to absorb sound.

The higher density materials possesses larger fiber surfaces per unit volume[57]. H. S. Seddeq [58] made a point that the higher fiber surface increases a material's friction loss, promoting more energy transformation from sound to heat energy.

A material's porosity is defined as the sound wave dissipation, which depends on the structural configuration involving pores or voids. The ratio (equation 2) of voids/holes to the total volume is the dominant factor affecting the material's ability to dissipate sound waves.

$$\text{Porosity (H)}: \frac{V_a}{V_m} \tag{2}$$

The V_a and V_m represent the volume of air in voids and total volume of material, respectively.

the principle of transmission path where the external sound waves strike to the porous material is similar for pores, granular, fibrous and cellular material, even though the porosity of the sound absorbing material involves multiple material configurations,. When the external sound waves strike the wall, the sound energy is converted to heat energy because of the pores and channels of the wall, which results in energy losses in air molecules. The active air molecules transmit to other air molecules contained in the pores and channels of porous material, giving rise to the vibration and energy losses. M. Crocker and J. Arenas [59] placed their focus on investigating the effects of different pore and channel diameters on energy transformation. They studied micro-perforated panels with diameters of 30mm and 60mm, respectively, and found a better absorption coefficient is achieved with a larger diameter. Different air gap diameters were investigated by M. Bilova and E. Lumitzer [60] to test their effects on sound transmission. The tested air gaps were behind the PUF absorption material with fixed diameter and acted as cavities allowing the sound waves to transmit and hit the rigid back panel.

Absorption materials are always applied as part of sandwich panels to improve the structural acoustic performance. M. P. Arunkumar et. al [61] studied the acoustic behavior of truss core sandwich panels based on its corresponding equivalent 2D model and enhanced the structural ability of sound insulation by adding the PUF foam into the core. The acoustic behavior of glass fiber assembly-filled honeycomb sandwich panels was experimentally tested by Y. Yang et. al [62] with respect to different filling shapes, fiber diameters, fiber contents, and air-layer distributions. The vibro-acoustic behavior of three foam-filled sandwich panels with different core shapes: hexagon, truss, and Z core, were studied by M. P. Aurnkumar et. al [63] with the equivalent theory. They

demonstrated smaller amplitude vibrations and desirable acoustic comfort can be achieved with foam-filled truss core sandwich panels. However, vibro-acoustic investigations of sandwich panels filled with wood-based material are rarely found in the literature. In this chapter, the effect of truss core sandwich panels filled with wood-based porous media on structural acoustic characteristics are discussed. The comparison between a PUF foam-filled truss core sandwich panel and wood board-filled truss core sandwich panel are conducted. The advantages of comparable sound insulation capability and environmental-friendly properties in wood board-filled truss core sandwich structures over their foam-filled counterpart can be observed. The significant fluid property which plays the most import role in vibro-acoustic responses and the function of absorption materials can be determined from the analysis of wood-based porous media with different fluid properties and wood-based porous medium-filled truss core sandwich panels with different face sheets.

4.2 Model establishment and numerical methodology

An equivalent theory, which is able to simulate the complex absorption medium-filled triangle honeycomb sandwich panel into a continuously orthotropic layer, is used to reduce pre- and post- simulation time and simplify the simulation procedure.

L and B [64] studied the flexural behavior of an orthotropic plate based on the general small-deflection theory. They used seven elastic constants (Figure) to describe the properties of the thick plates by comparing the behavior of a unit cell with the behavior of an element of an orthotropic thick plate. They are D_x, D_y (bending stiffness), ν_x, ν_y (bending Poisson ration), D_{xy} (twisting stiffness), D_{Qx}, ands D_{Qy} (transverse shear

stiffness). The equivalent properties of a foam-filled truss core sandwich panel are obtained based on the force-distortion relationship investigated by L and B. An assumption established in the equivalent theory is that the foam and truss core can be summed with the relevant equivalent stiffness properties of the foam. Equations used to calculate the equivalent stiffness properties are summarized as:

$$D_x = \frac{E_x h^3}{12};\ D_y = \frac{E_y h^3}{12};\ D_{xy} = \frac{G_{xy} h^3}{6}$$

$$D_{Qx} = k^2 G_{xz} h;\ D_{Qy} = k^2 G_{yz} h. \quad (1)$$

Where E_x and E_y are the elastic moluli and G_{xy}, G_{xz} and G_{yz} are the shear moduli. k^2 denotes the transverse shear correction factor with the value being $\pi^2/12$ [29].

The truss core dimensions are expressed in the Figure, in which the unit is symmetrical with respect to a vertical direction and the panel is symmetrical in terms of the middle layer because the thickness of the two face sheets are identical. The unit truss core elastic constants of the unit truss core are formulated as follows:

$$D_x = E(I_c + \frac{td^2}{2}) + E_{Fo}(I_t - (I_c + \frac{td^2}{2}))$$

$$D_y = \frac{EI_f}{1 - \frac{\gamma^2 I_c}{I_c + I_f}} + E_{fo}\frac{d_c^3}{12}$$

$$D_{xy} = \frac{1}{2}Gtd^2$$

$$D_{Qx} = Gt_c \frac{\frac{d^2 t}{pst_c} + \frac{1}{6}(\frac{d_c}{p})^2}{\frac{t}{t_c} + \frac{sd_c}{3pd}} + G_{fo} d_c$$

$$D_{Qy} = \frac{1}{\frac{\delta_y}{d} + \frac{\delta_z}{p}} + G_{fo} d_c \qquad (2)$$

Where δ_y and δ_c are deflection parameters developed by Lok and Cheng; I_c and I_f represent the moments of inertia per unit width of the truss core cross section in the yz plane:

$$I_c = \frac{lt_c d_c^2}{12p}, \quad I_f = \frac{t_f d^2}{2} \qquad (3)$$

An orthotropic equivalent 2D plate can be extracted based on equivalent theory. The 2D plate is analysed and meshed with the layer structural element method in hypermesh, then imported into Actran for investigation of its vibro-acoustic behavior. In Actran, the 2D plate model is given the same thickness as the original 3D model and given the property of visco-elastic thin shells, which present a component with one very small dimension and two larger dimensions. Thin shells are elements having a dimension one unit lower than the dimension of space (shown in the table 4.2):

Table 4.2 Supported topologies in Actran

3D Computations	
QUA04	Yes
QUA08	No
TRI03	Yes
TRI06	No

Each node supports six degrees of freedom with displacement representing x, y and directions and rotation denoting x, y, and z direction.

The simulation methodology for free and forced vibration responses and the STL is similar to that shown in Chapter 3. The clamped boundary condition is applied in the simulation:

$$\mathrm{x} = 0, \mathrm{a}: \mathrm{w} = 0, \theta_x = \frac{\partial w}{\partial x} = 0$$

$$\mathrm{y} = 0, \mathrm{b}: \mathrm{w} = 0, \theta_y = \frac{\partial w}{\partial y} = 0 \quad (4)$$

4.3 Validation studies

4.3.1 Validation of free vibration results with simulation and theory

A comparison between the simulated results and theoretical results analyzed by L and C [65] is considered in order to validate the proposed method to predict the free vibration of a foam-filled truss core sandwich panel. They studied a truss core sandwich panel of size 1.2m*2m with 8 identical triangle cores inside (Fig.4.3.1 a). The dimensions and mechanical properties are $p = 75mm, f_0 = 25mm\,, d = 46.75mm,\ f_t = t_c = 3.25mm,\ E = 80GPa,\ \nu = 0.3,\ \rho = \frac{2700kg}{m^3}$. The free vibration frequencies obtained from Actran based on 3D and 2D models match well with the frequencies analyzed by L and C as seen in Table 4.3.1. Free vibration mode shapes obtained from Actran for 3D and 2D models are generated and compared as shown in Fig. 4.3.2, which represent the modes shapes in the low and high frequency ranges.

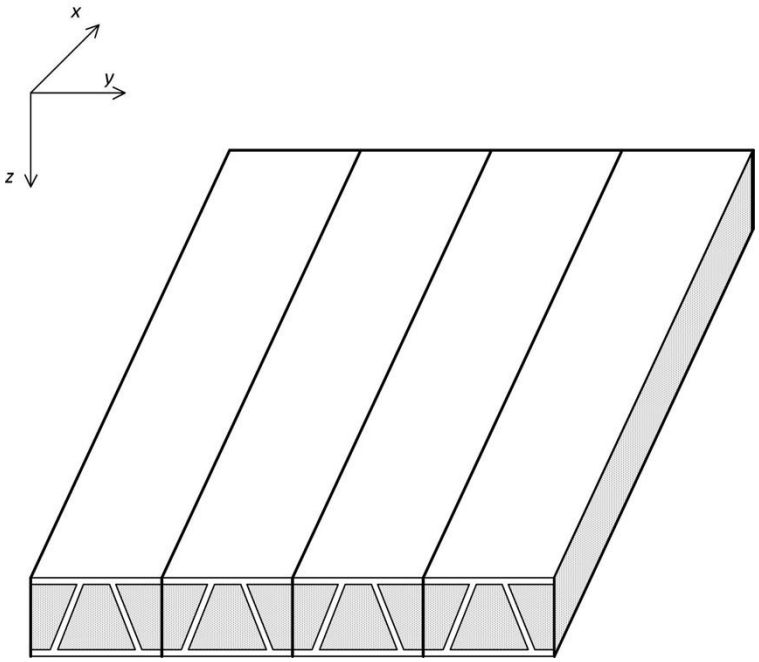

Fig.4.3.1 a Dimensions of the truss core sandwich panel

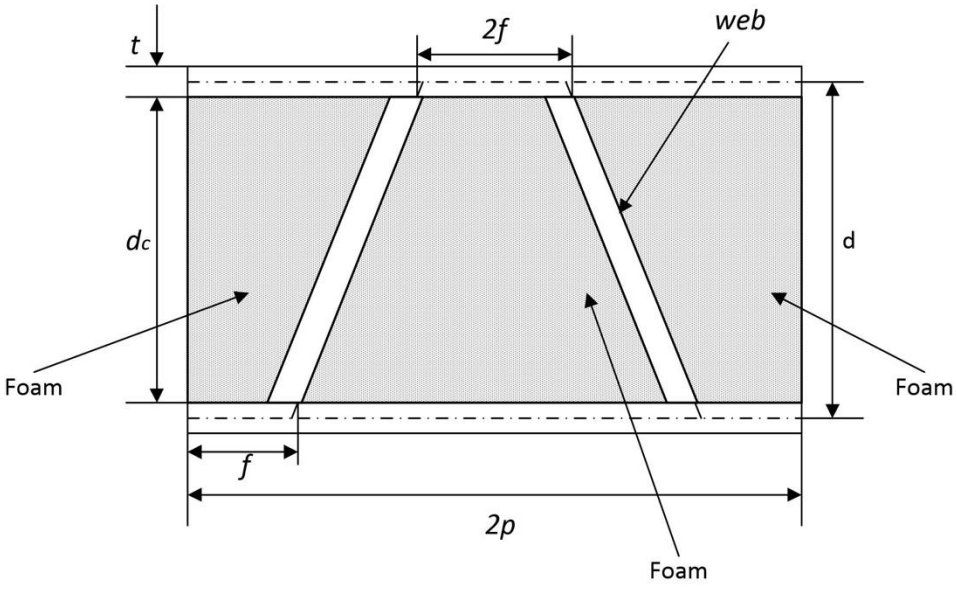

Fig.4.3.1 b Dimensions of the unit cell truss core

Table 4.3.1 Comparison of natural frequency between proposed results and theoretical results

Mode	Free vibration frequency (Hz)			
	3D model		Equivalent 2D model	
	Lok & cheng	Present	Lok & Cheng	Present
(1,1)	139.3	148.0862796	138.7	144.5002535
(2,1)	213.6	225.7780996	211.1	216.4666503
(1,2)	297.4	279.2941665	294.2	300.3630465
(3,1)	290	287.7568215	294.8	311.5483172
(2,2)	348.1	336.1947347	352.1	368.2053017
(4,1)	382	394.5583602	378.9	387.1520607
(3,2)	426.2	417.5623148	431.2	448.4886458
(5,1)	466.2	453.4376631	463.2	475.1387591
(4,2)	501.6	512.3370564	517.7	537.473799
(1,3)	509.5	515.9774171	521.3	552.6227242

4.3.2 Comparison of radiation modes predicted by 3D and 2D finite element models for the panel.

Mode	3D FE model	Equivalent 2D FE model
(1, 1)	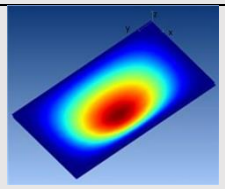	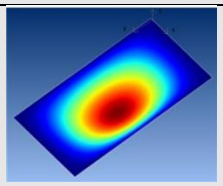
(1, 2)	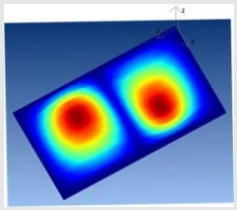	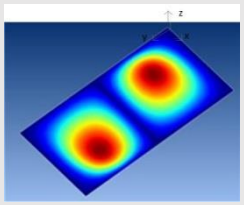
(2, 2)	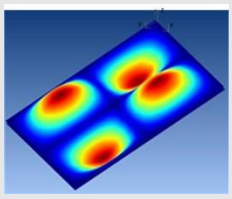	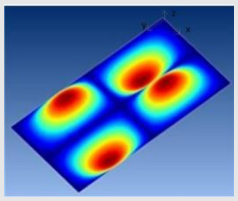
(3, 2)	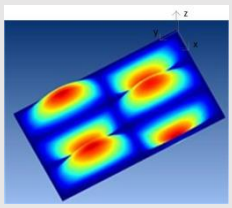	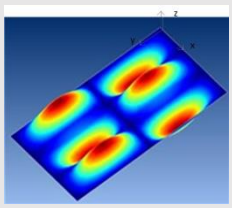
(4, 2)	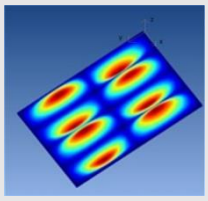	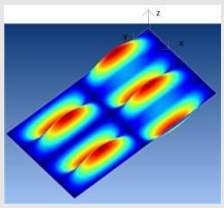

Fig. 4.3.2 vibration modes comparison

4.3.3 Validation of the STL evaluation

The available data from the experiment applied by C & K [17] is assessed to validate the proposed method of predicting the STL. L & K analyzed a sandwich panel of size 0.303 m*0.203 m with the top and bottom face sheets having a thickness 0.5 mm and a core thickness of 2 mm. The density of the face sheet and core material is 2720 kg/m^3 and 1.60 kg/m^3, respectively. The Young's modulus and shear modulus of the face sheet and core material are given as 73.2 GPa and 4.12 GPa, respectively. The Poisson's ratios for the face sheet and core material are given as 0.33 and 0.4, respectively. The sound transmission loss predicted using the proposed method agrees with the experimental and analytical data, as seen in Fig. 6.

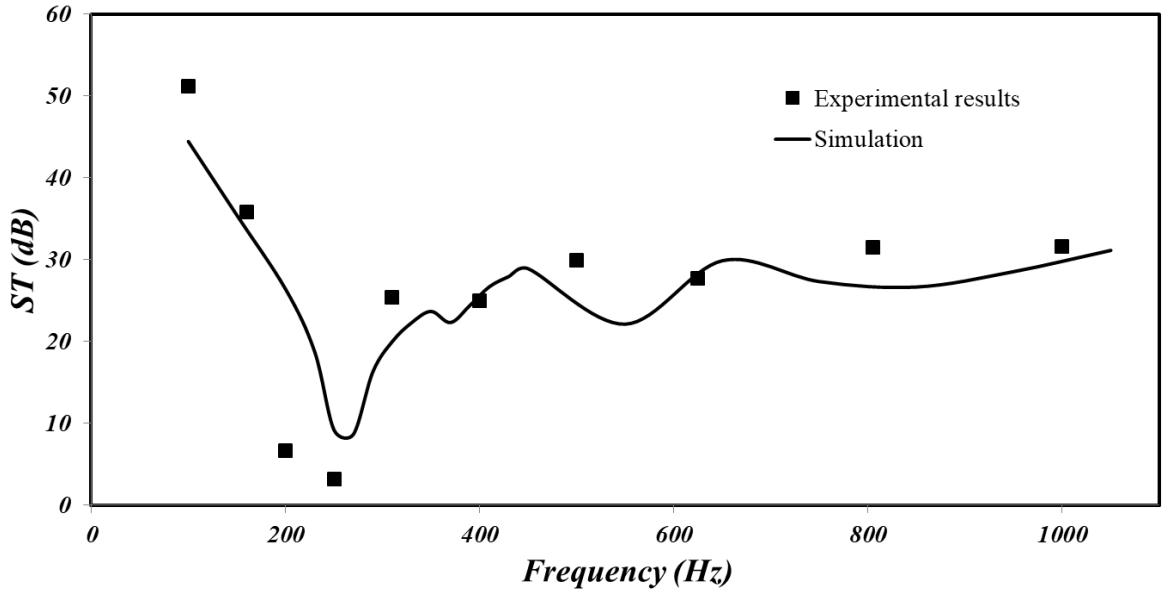

Fig. 4.3.3 Sound transmission loss validation

4.4 Numerical results and analysis

4.4.1 Acoustic analysis based on mineral-porous and wood-based porous materials

Two typical porous materials, PUF foam and wood board porous media, are selected to investigate the effect of filling material on vibro-acoustic behavior.

Table 4.4.1 Mechanical properties for PUF foam and wood board porous medium

Porous material	Porosity	Resistivity	Tortuosity
PUF foam	0.97	22000	1.38
Wood board porous medium	0.4	670000	200

The sound insulation of truss core sandwich panels is improved with the porous medium filled in the core. The principle of sound insulation of porous media depends on the properties of the porous material, such as the porosity, airflow resistivity, and tortuosity, which can somehow decrease the transmission speed of sound in the material and increase energy consumption. Adding the porous medium makes the sandwich panel appear acoustically thicker. The PUF foam, which has been widely used in industry, as well as wood board porous media, which possesses low cost and environmental-friendly characteristics, is placed under study. The largest average root mean square amplitude occurred in the wood board-filled truss core sandwich panel and the sound power radiated from the wood board-filled truss core sandwich panel in the first resonance frequency was the largest. This is due to a closing frequency trend between the external sound wave frequencies and structural natural frequencies, resulting in an acceleration of

sound transmission in solid material. The difference among the panels in the low frequency range cannot be clearly recognized and the gaps between the three panels are not wide. The STL in the truss core sandwich panel filled with wood board material is the highest in the stiffness-controlled region due to its high stiffness, and shows a better sound insulation property at high frequency (≥1000Hz) as well, which agrees with the mass law. The truss core sandwich panel filled with UPF foam exhibits a stable increase in its STL property, especially at resonant frequencies, diminishing the side-effect of the resonant vibration. According to the 1/3 octave bank graphic, sound insulation keeps continuously increasing with the increasing of airflow resistivity properties, which implies the airflow resistivity, plays a dominant factor in sound insulation.

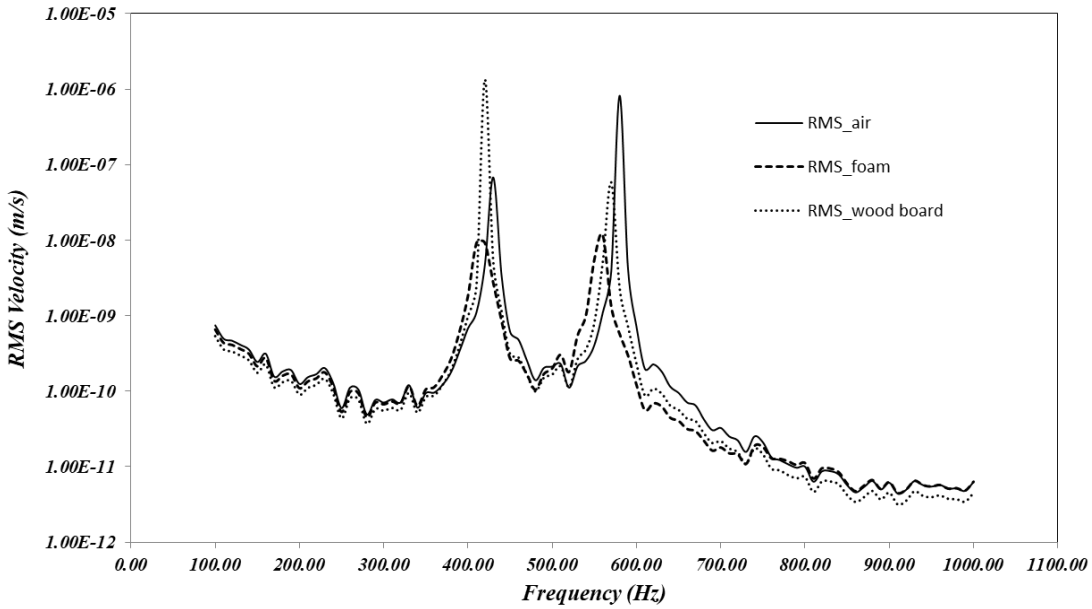

Fig. 4.4.1 a Vibration Responses

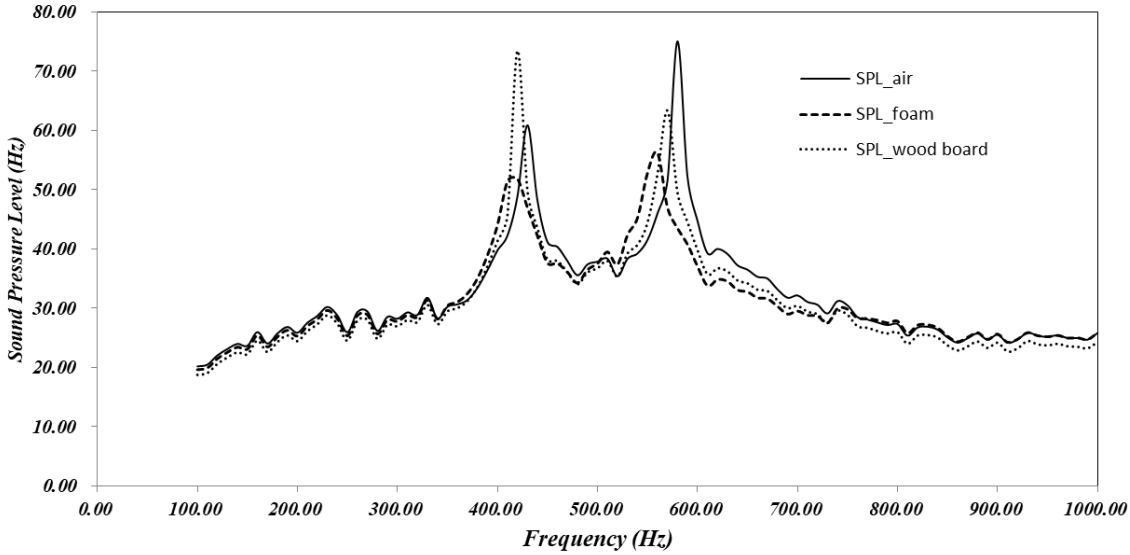

Fig. 4.4.1 b Sound Pressure Level

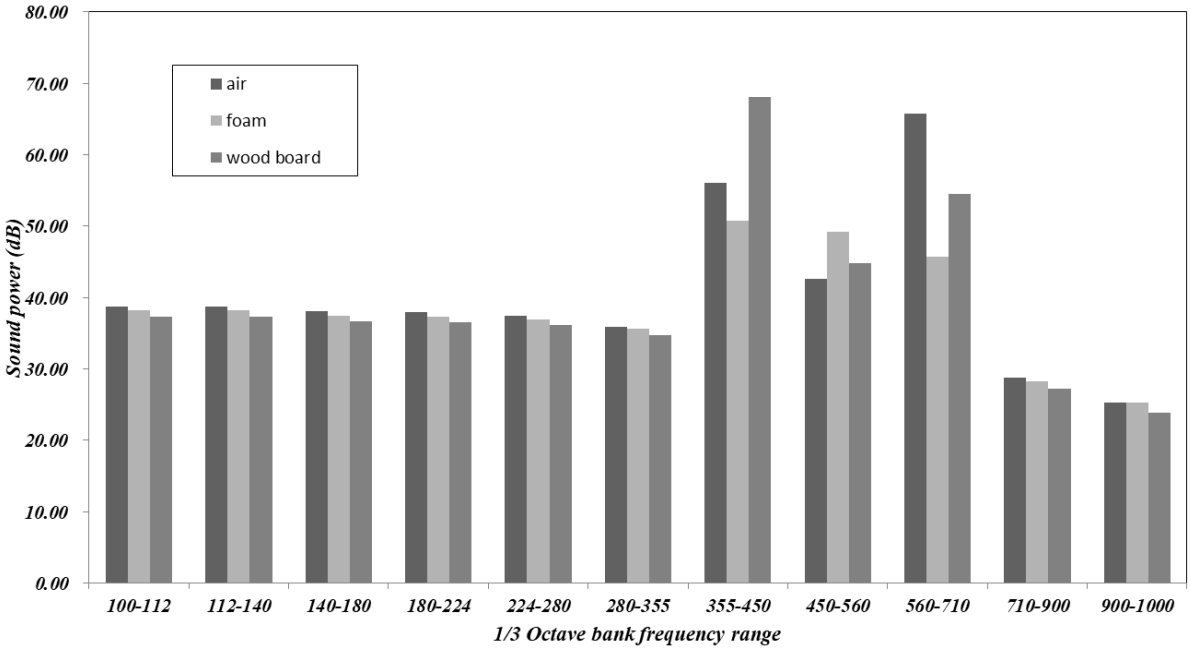

Fig. 4.4.1.c 1/3 Octave bank frequency range

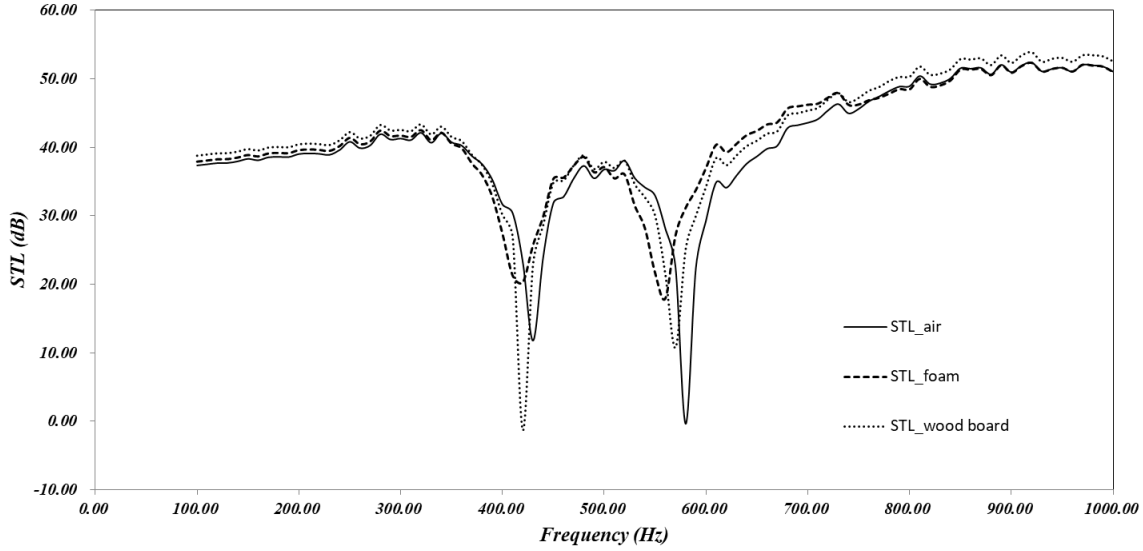

Fig.4.4.1 d Sound Transmission Loss

4.4.2 Acoustic analysis based on wood-based absorption materials

The truss core sandwich panel filled with wood-based medium is investigated. Two wood-based media with various porous characteristics, wood board and wood shaving, are applied and studied for various manufacturing processes. Wood board is typically made of mineral fibers to make a porous bat or compressed panel and possesses a high density, whereas wood shaving is much less dense in structure. The characteristics of wood-based porous media are investigated including airflow resistivity, porosity, and tortuosity. Reflected sound power from the panel cannot be clearly recognized in the low frequency range. In the resonant frequency range, acoustic performance in the empty sandwich panel is better than in the wood board sandwich panel and wood shaving sandwich panel. This is because a dramatic vibration is generated due to the closing frequency trend between the external sound wave frequencies and structural natural frequencies. This leads to a high sound power transmission. Sound transmission in solid materials accelerates the sound power transmission. However, the gaps among the three are narrow, as shown in Fig. 4.4.2.c. This means the sound power of the wood-based-porous-medium-filled truss core sandwich structure radiated from the panel is still within an acceptable range. By comparing the effects of the absorption material properties, it becomes apparent wood board plays a significant role in noise control which mainly relies upon high resistivity properties.

Table. 4.4.2 Mechanical properties for different wood-based porous medium

Porous material	Porosity	Resistivity	Tortuosity
wood board	0.4	670000	200
wood shaving	0.6	115000	10

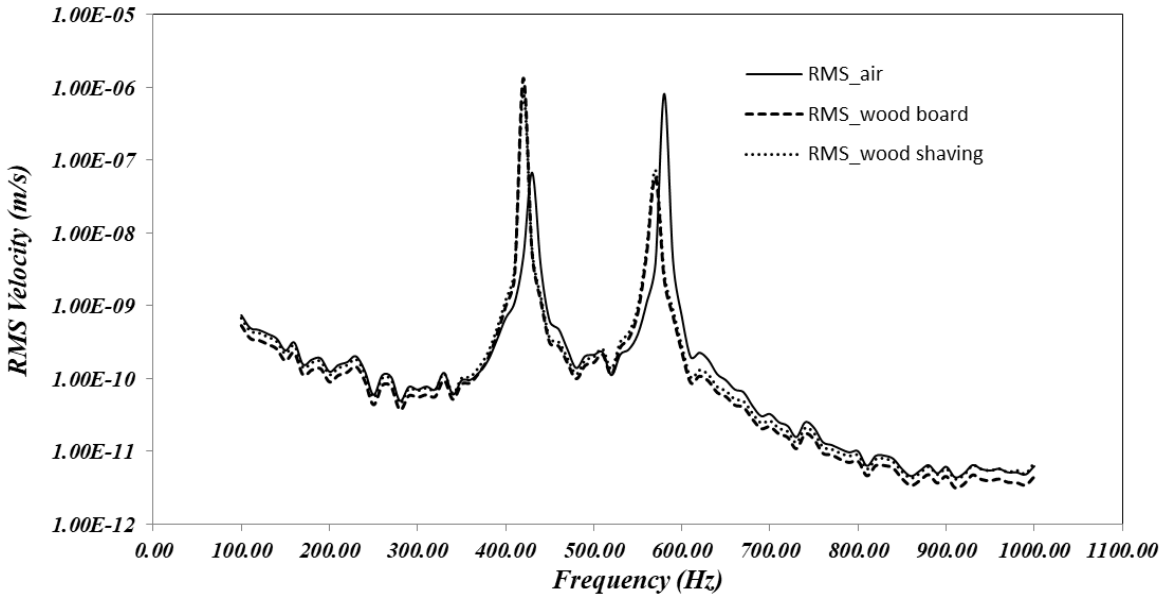

Fig. 4.4.2 a Vibration Responses

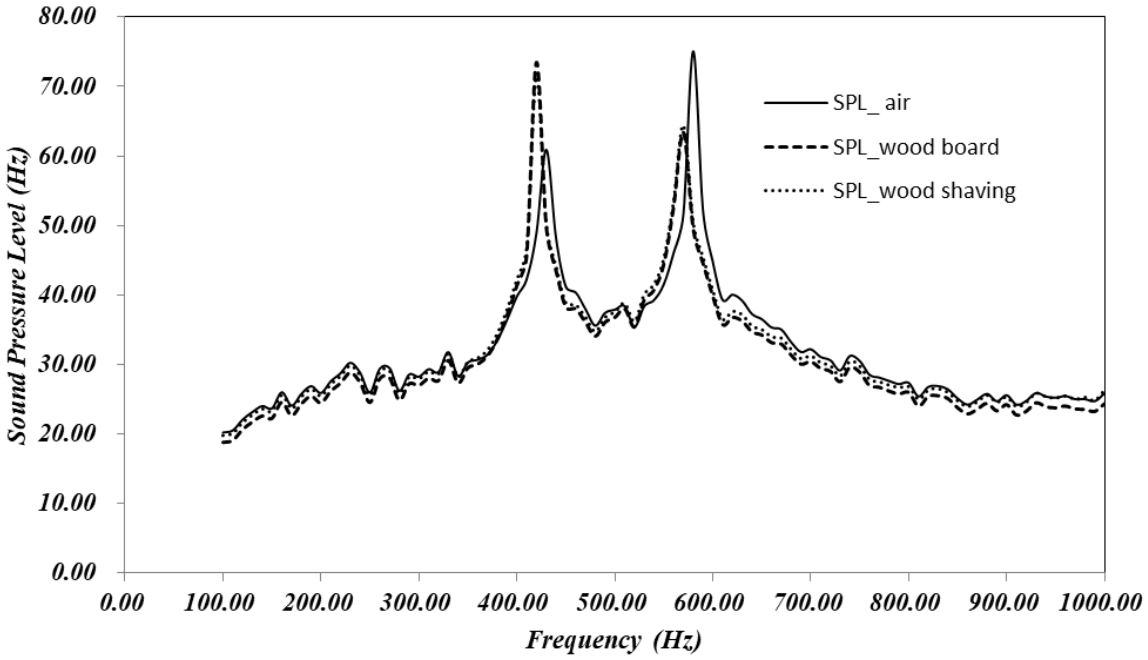

Fig. 4.4.2 b Sound Pressure Level

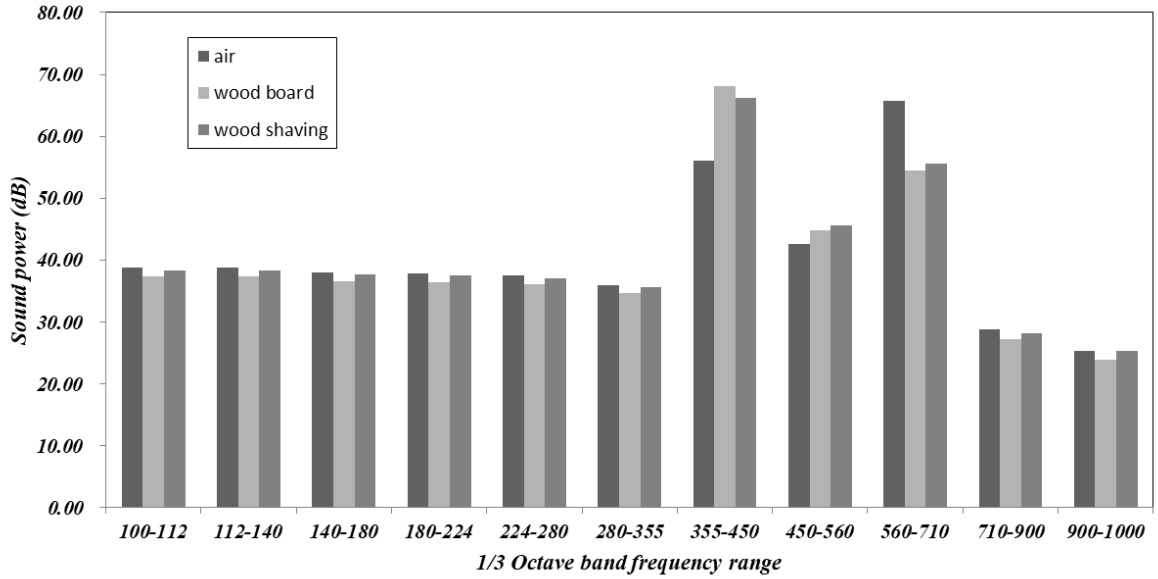

Fig. 4.4.2.c 1/3 Octave band frequency range

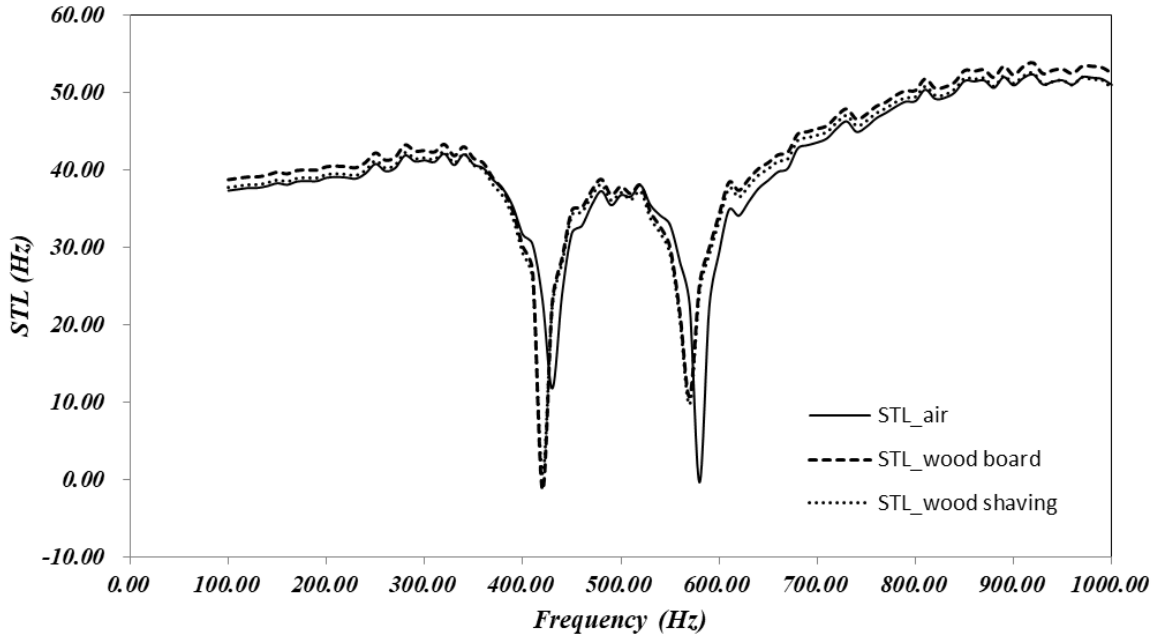

Fig. 4.4.2 d Sound Transmission Loss

4.4.3 Acoustic analysis based on different material of face sheets

A comparison of various material face sheets used in truss core sandwich panels is conducted. Three materials with different stiffness and density properties, aluminum, titanium, and epoxy-carbon, are selected to investigate the acoustic performance of the sandwich panel. The epoxy carbon truss core sandwich panel reflects the highest sound power in the low frequency range due to its comparatively high stiffness (add graphic). The titanium truss core sandwich panel shows the highest STL in the stiffness-controlled region because of high density (add graphic). However, the STL gap in three truss core sandwich panels is not wide in the 1/3 octave frequency range graphic. The differences in STL can be recognized in the mass-controlled frequency range (middle frequency range), and the titanium truss core sandwich panel shows remarkable advantages in high frequency noise control.

Table 4.4.3 Mechanical properties for different face sheets

Face sheets	Young's modulus(GPa)	Density (kg/m^3)
Aluminum	72	2700
Titanium	120	4500
Epoxy carbon	143	1600

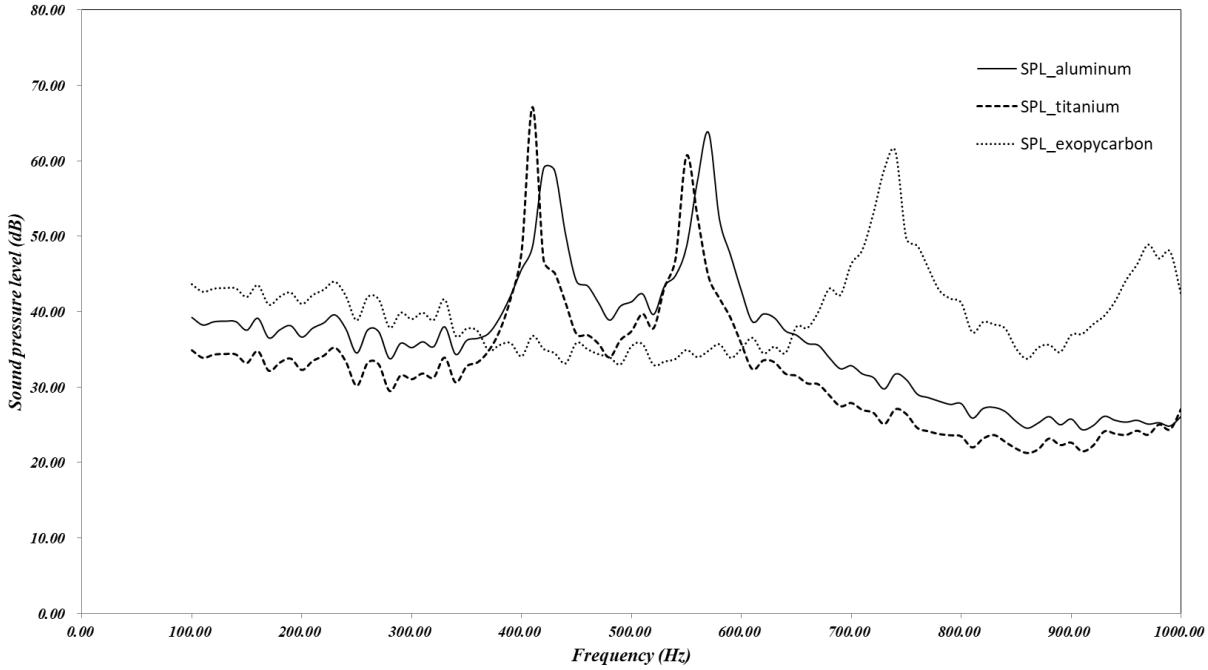

Fig. 4.4.3 a Sound Pressure Level

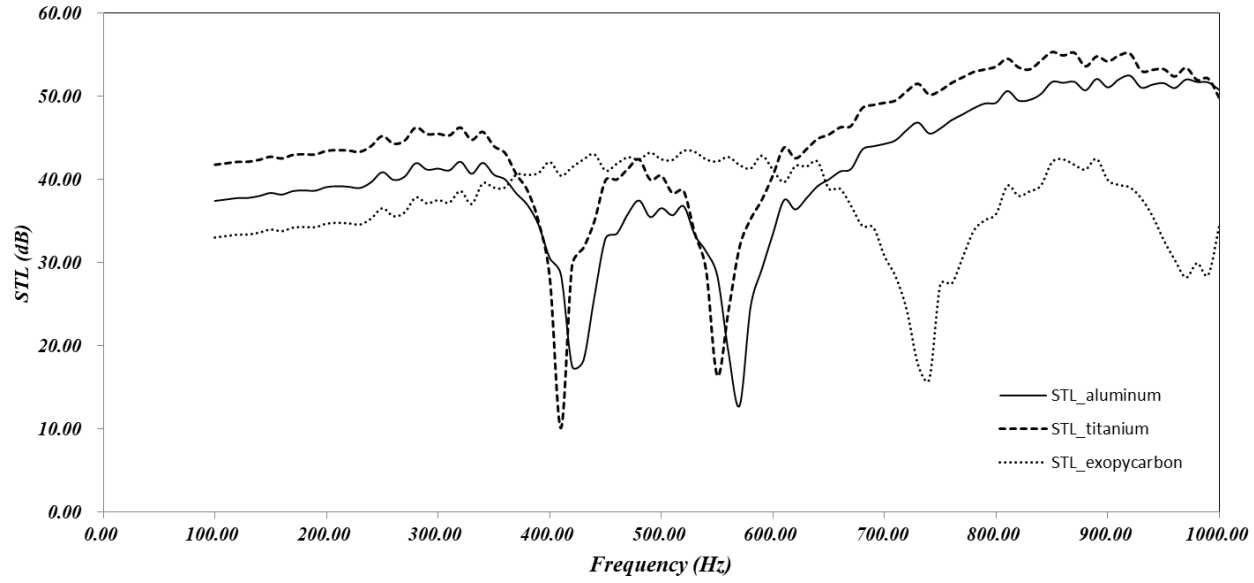

Fig. 4.4.3 b Sound Transmission Loss

CHAPTER 5 CONCLUSION AND DISCUSSION

This research intended to numerically investigate an aluminum honeycomb core and fabric-reinforced graphite face sheet sandwich panel with respect to vibro-acoustic and sound transmission losses. Due to desirable acoustic performance in the low frequency range, with less space-occupation and light-weight design, the FRG composite honeycomb sandwich panel is suggested as an alternative to the conventional aluminum honeycomb sandwich panel and FRP honeycomb sandwich panel.

A wood-based-porous-medium-filled truss core and epoxy-carbon face sheet sandwich panel is put forward as a replacement for the widely applied PUF foam-filled truss core with aluminum face sheet sandwich panel. This is due to its excellent sound insulation in the low frequency range with low cost, light-weight, and environmental-friendly design. With the investigations conducted in the research, the following conclusions have been reached:

1. The FRG composite honeycomb sandwich panel possesses the lowest radiation modes and highest stiffness and density properties compared with conventional aluminum honeycomb sandwich and FRP composite honeycomb sandwich panels. This creates the most stable radiation sound power level and STL curve. A desirable acoustic performance can be achieved as a result.
2. The CCCC boundary condition plays a significant role in the structural mechanical properties, enhancing the stiffness property of the FRG honeycomb sandwich panel. The FRG honeycomb sandwich panel, under the CCCC boundary condition, has the lowest number of radiation modes. A high acoustic

performance with a relatively stable trend in the sound power level and the STL is achieved.

3. With regard to the effects of different geometric properties of a honeycomb core on the radiated sound power and STL behavior, the variation from the honeycomb core height affects the acoustic performance more significantly than the honeycomb cell size. Structural acoustic properties are more sensitive changes in the height of the face sheets, than core height, which agrees with the mass law.
4. The FRG panel possesses significant advantages in the acoustic properties over the conventional aluminum sandwich panel and FRP composite honeycomb sandwich panel. The design is focused on the vibrational and acoustic behaviors of the sandwich panels. The FRG panel can be used to replace the other two honeycomb structures that were investigated.
5. The truss core sandwich panel filled with a wood board porous medium achieves a better STL characteristic in the stiffness-domain and mass-domain regions compared to the PUF foam. Even though the acoustic behavior of a wood-based medium filled honeycomb panel is not as stable as a PUF foam-filled honeycomb sandwich panel for resonant frequencies, a compatible sound insulation property is still within expectations.
6. The absorption material can relieve the side-effect of resonant vibration and improve the overall sound insulation property, whereas the mechanical properties of a honeycomb sandwich structure are not affected. This can be reflected by the vibro-acoustic behavior of wood-based-medium-filled truss core sandwich panel with different material face sheets.

7. The airflow resistivity property plays a dominant role in vibro-acoustic behavior based on the investigation between wood board porous media and wood shaving porous media.
8. The wood-based-porous-medium-filled truss core and carbon-epoxy face sheets achieve a better acoustic performance in the low frequency range. Titanium face sheets and the wood-based-porous-medium-filled truss core show an increasing trend in the STL curve in the high frequency range due to its high density, which agrees with the mass law.
9. The present approach can be useful when evaluating and selecting honeycomb sandwich panels when the vibrational and acoustic behaviors of the panels are considered.

CHAPTER 6 FUTURE WORK

In future research, the vibro-acoustic behavior of porous medium-filled honeycomb sandwich panels may be investigated as a function of sound radiation responses, STL behavior of porous medium-filled honeycomb sandwiches, and various degrees of vacuum .

The sound cannot be propagated in extreme vacuum conditions. In addition, porous media are commonly used to improve structural sound insulation. A method for sound insulation, which is a combination of porous media filled with various vacuums, is suggested based on the two fundamental theories. The equivalent model for the porous medium-filled honeycomb sandwich panel is required to be identified, which can simplify simulations and save the pre- and post- simulation times. A fundamental theoretical background of structural mechanics is needed to derive an equivalent model to figure out the relationship between airflow and porous media. The effect of degrees of vacuum on radiation responses and STL behavior can be obtained from corresponding fluid properties, such as air density, airflow resistivity, and porosity. The equivalent orthotropic panel is mathematically modeled by means of the boundary and shell element method. The equivalent model's forced vibration responses are used as input for the Rayleigh integral to obtain its corresponding radiated sound power. Finally, the STL is calculated with a constant incident sound power.

The expected results are roughly demonstrated as the sound insulation properties of porous medium-filled honeycomb sandwich panels can be increased with increasing of

degrees of vacuum in a given region and decreased after the outside the region. Possible factors require investigation and the optimal vacuum is needed.

CHAPTER 7 BIBLIOGRAPHY

[1] J. P. Nunes & J. F. Silva, "Sandwiched composites in aerospace engineering", *Advanced Composite Materials for Aerospace Engineering*, (2016), 129-174.

[2] R. Kopp, C. Abratis & M. Nutzmann, "Lightweight sandwich sheets for automobile applications", *Production Engineering Research and Development*, 11.2 (2004), 55-60.

[3] S. Zhe, "Application of composite sandwich structure in automobile", *Fiber Reinforced Plastics*, 4 (1997).

[4] H. Liu, J. Wei & Z. Qu, "Prediction of aerodynamic noise reduction by using open-cell metal foam", *Journal of Sound and Vibration*, 331.7 (2012), 1483-1497.

[5] V. Crupi, G. Epasto & E. Guglielmino, "Impact response of aluminum foam sandwiches for light-weight ship structures", *Metals*, 1.1 (2011), 98-112.

[6] S. Rao, K. Jayaraman & D. Bhattacharyya, "Short fiber reinforced cores and their sandwich panels: Processing and evaluation", *Composites Part A*: Applied Science and Manufacturing, 42.9 (2011), 1236-1246.

[7]. R. Vaicaitis, F. W. Grosveld & J. S. Mixson, “Noise Transmission through Aircraft Panels”, *Journal of Aircraft*, 22.4 (1985), 303-310.

[8]. R. Vaicaitis & J. S. Mixson, “Theoretical Design of Acoustic Treatment for Noise Control in a Turboporp Aircraft”, *Journal of Aircraft*, 22.4 (1985), 318-324.

[9]. P. K. Mallick, “Fiber-Reinforced Composites: Material, Manufacturing and Design”, *CRC press* (2007).

[10] M. P. Arunkumar. J. Pitchaimani, K. V. Gangadharan & M. C. Leninbabu, “Vibro-acoustic response and sound transmission loss characteristics of truss core sandwich

panel filled with foam", *Aerospace Science and Technology*, 78 (2018), 1-11.

[11] Y. Yang, B. Li, Z. Chen, N. Sui, Z. Chen, M. U. Saeed, Y. Li, R. Fu, C. Wu & Y. Jing, "Acoustic properties of glass fiber assembly-filled honeycomb sandwich panels", *Composites Part B*, 96(2016), 281-286.

[12]. P. Wennhage, "Weight optimization of large scale sandwich structures with acoustic and mechanical constraints", *Journal of Sandwich Structure & Materials*, 5 (2003):253–266.

[13]. O. Onursal & C. Mehmet, "Design of a single layer micro-perforated sound absorber by finite element ayalysis", *Applied Acoustics*, 71.1 (2010), 79-85.

[14]. W. Yonghua, Z. Chengchun, R. Luquan, I. Mohamed, G. Marie-Annick & B. Olivier, "Sound absorption of a new bionic multi-layer absorber", *Composite Structures*, 108 (2014),400-408.

[15] N. Indrianti, N. B. Biru & T. Wibawa, "The development of compressor noise barrier in the assembly area: (Case study of PT Jawa Fuini Lestari)", *Procedia CIRP* (2016), 705-710.

[16] J. A. Scales & R. Snieder, "What is noise?" *Geophysics*, 63 (1998), 1122–1124.

[17] A. R. Mohanty. & . S. Fatima, "An overview of automobile noise and vibration control", *Noise & Vibration Worldwide* (2013), 10-19.

[18] D. Zhou, Z. Luo, M. Fang, J. Jiang, H. Chen, D. Sha & M. Lu, "Numerical study of the movement of fine particle in sound wave field", *Energy Procedia* (2015), 2415-2420.

[19] C. H. Hansen, "Fundamental of Acoustics", University of Adelaide (2001), Adelaide.

[20] B. W. Niebel & A. Freivalds, " Niebel's methods, standards, and work design", 12ed.

Europe: McGraw-Hill Education (2008).

[21] M. Crocker & J. Arenas, “Handbook of Noise and Vibration Control”, *New York: John Wiley and Sons* (2007).

[22] S. W Rienstra. & A. Hirschberg, “An Introduction to Acoustics”, *Eindhoven University of Technology* (2016).

[23] M. Bruneau, "Fundamentals of Acoustics", *ISTE Ltd* (2006), Great Britain.

[24] P. N. Breysse & P. S. Lees, “Noise”, *The Johns Hopkins University* (2006).

[25] J. Jiang & L. Yun, “Review of active noise control techniques with emphasis on sound quality enhancement”, *Applied Acoustics*, 136 (2018), 139-148.

[26] R. F Barron, “Industrial noise control and acoustics”,(2003).

[27] P. H. Parkin, H. R. Humphreys & Cowell JR, “Acoustics, noise and buildings”, *London: Faber & Faber* (1979).

[28] M. A. Kuczmarski & J. C. Johnston, "Acoustic Absorption in Porous Materials", *NASA, Ohio* (2011).

[29] H. P. Degischer., & B. Kriszt, "Handbook of Cellular Metals: Production, Processing, Applications”, (2002).

[30], T. D., “Springer Handbook of Acoustics”, *Springer* (2007), New York.

[31] M. P. Arunkumar & J. Pitchaimani. "Sound transmission loss characteristics of sandwich aircraft panels: Influence of nature of core", *Journal of Sandwich Structures & Materials*, 19 (2017), 26-48.

[32] D. Griese, J. D. Summers, & L. Thompson. "The effect of honeycomb core geometry on the sound transmission performance of sandwich panels", *Journal of Vibration and Acoustics*, (2014).

[33] I. Prasetiyo & D. Thompson, "Study of the effect of finite extent on sound transmission loss of single panel using a waveguide model", *Acoustics* (2012).

[34] J. K. Paik, A. K. Thayamballi & G. S. Kim, "The strength characteristics of aluminum honeycomb sandwich panels", *Thin-walled structures*, 35 (1999), 205-231.

[35] S. Marburg & B. Nolte, "Computational acoustics of noise propagation in fluids: finite and boundary element methods", *Berlin: Springer*, 578(2008).

[36] S. M. Kirkup & D. J. Henwood, "Computational solution of acoustic radiation problems by kussmaul's boundary element method", *Journal of Sound and Vibration*, 158.2 (1992): 293-305.

[37] S. M. Kirkup, "Computational solution of the acoustic field surrounding a baffled panel by the Rayleigh integral method", *Applied Mathematical Modeling*, 18.7 (1994), 403-407.

[38] J. W. Rayleigh, "The Theory of Sound", *Dover* (1954), New York, USA.

[39] S. M. Kirkup, "The computational modeling of acoustic shields by the boundary and shell element method", *Computers & Structures*, 40.5 (1991), 1177-1183.

[40] C. Lee & K. Kondo, "Noise transmission loss of sandwich plates with viscoelastic core", *40th Structures, Structural Dynamics, and Materials Conference and Exhibit* (1999).

[41] M. P. Aurnkumar, J. Pitchaimani, K. V. Ganfadharan & M. C. Lenin Babu, "Sound transmission loss characteristics of sandwich aircraft panels: Influence of nature of core", *Journal of Sandwich Structures & Materials*, 19 (2017), 26-48.

[42]. M. P. Arunkumar, M. Jagadeesh, J. Pitchaimani, K. V. Gangadharan & M. C. Lenin Babu, "Sound radiation and transmission loss characteristics of a honecycomb

sandwich panel with composite facings: Effect of inherent material damping", *Journal of Sound and Vibration*, 383 (2016), 221-232.

[43]. V. D'Alessandro, G. Petrone & F. Franco, "A review of the vibroacoustics of sandwich panels: models and experiments", *Journal of Sandwich Structures & Materials*, 15 (2013), 541–582.

[44] G. Squicciarini, D. J. Thompson & R. Corradi, "The effect of different combinations of boundary conditions on the average radiation efficiency of rectangular plates", *Journal of Sound and Vibration*, 333.17 (2014), 3931-3948.

[45] A. Boudjemai, R. Amri, A. Mankour, H. Salem, M. H. Bouanane & D. Boutchicha, "Modal analysis and testing of hexagonal honeycomb plates used for satellite structural design", *Materials & Design*, 35 (2012), 266-275.

[46] I. Aydincak, "Investigation of design and analyses principles of honeycomb structures", Master of Science Project Thesis, *Middle East Technical University* (2007).

[47] L. Cremer & M. Heckl,"Structure-borne sound: structural vibrations and sound radiation at audio frequencies", *Springer Science & Business Media* (2013).

[48] Z. Ran & C. J. Malcolm, "Sound transmission loss of foam-filled honeycomb sandwich panels using statistical energy analysis and theoretical and measured dynamic properties", *Journal of Sound and Vibration*, 329 (2010), 673-686.

[49] F. Liying & W. Weiyang, "Equivalent Calculation and Experiment Research on the Honeycomb Sandwich Plates Used in Satellite", *Science Technology and Engineering*, 8.23 (2008), 6429-6432.

[50] X. Xia, L. Jin, & W. Yangbao, "The Equivalent Analysis of Honeycomb Sandwich

Plates for Satellite Structure", *JOURNAL-SHANGHAI JIAOTONG UNIVERSITY-CHINESE EDITION*, 37.7 (2003), 0999-1001.

[51] L. Hao, L. Geng, M. Shangjun, & L. Wenbin, "Dynamic analysis of the spacecraft structure on orbit made up of honeycomb sandwich plates". In Computer Science and Automation Engineering (CSAE), *IEEE International Conference* (2001), IEEE, 83-87.

[52] J. K. Paik, A. K. Thayamballi, & G. S. Kim, "The strength characteristics of aluminum honeycomb sandwich panels", *Thin-walled structures*, 35 (1999)., 205-231.

[52] N. Buannic, P. Cartraud, & T. Quesnel, "Homogenization of corrugated core sandwich panels", *Composite structures*, 59 (2003), 299-312.

[53] O. Doutres & N. Atalla, "Sound Absorption Properties of Functionally Graded Polyurethane Foams," New York (2012).

[54] A. Zaidi, A. Mujuhid, M. I. Ghazali, M. N. Yahya & M. Ismail, "Investigation on Sound Absorption of Rice-Husk Reinforced Composite", (2009).

[55] F. Shahani, P. Soltani & M. Zarrebini, "The Analysis of Acoustic Characteristics and Sound Absorption Coefficient of Needle Punched Nonwoven Fabrics", *Journal of Engineered Fibers and Fabrics*, 9 (2014), 84-92.

[56] M. I. A. Abdalla, "Treatment the Effects of Studio Wall Resonance and Coincidence Phenomena for Recording Noisy Speech Via FPGA Digital Filter", *Journal of Telecommunication*, 2 (2010), 42-48.

[57] Y. E. Lee & C. W. Joo, "Sound Absorption Properties of Thermally Bonded Nonwovens based on Composing Fibers and Production Parameters", *Journal of Applied Polymer Science* (2004), 2295–2302.

[58] H. S. Seddeq, "Factors Influencing Acoustic Performance of Sound Absorptive Material", *Australian Journal of Basic and Applied Sciences* (2009), 4610-4617.

[59] M. Crocker & J. Arenas, “Handbook of Noise and Vibration Control”, (2007).

[60] M. Bilova & E. Lumitzer, "Acoustical Parameter of Porous Material and their Measurement", Acta Technica Corviniensis (2011), 39-42.

[61] M. P. Arunkumar, J. Pitchaimani, K. V. Gangadharan & M. C. Leninbabu, “Vibro-acoustic response and sound transmission loss characteristics of truss core sandwich panel filled with foam”, *Aerospace Science and Technology*, 78(2018), 1-11.

[62] Y. Yang, B. Li, Z. Chen, N. Sui, Z. Chen, M. U. Saeed, Y. Li, R. Fu, C. Wu & Y. Jing, “Acoustic properties of glass fiber assembly-filled honeycomb sandwich panels”, *Composites Part B*, 96 (2016), 281-286.

[63] M. P. Arunkumar, J. Pitchaimani, K. V. Gangadharan & M. C. Leninbabu,”Influence of nature of core on vibro acoustic behavior of sandwich aerospace structures”, *Aerospace Science and Technology*, 56 (2016), 155-167.

[64] C. Libove & S. B Batdorf, “A general small-deflection theory for flat sandwich plates”, *NATIONAL AERONAURICS AND SPACE ADMINISTRATION WASHINGTON DC* (1948).

[65] T. Lok & Q. Cheng, “Free vibration of clamped orthotropic sandwich panel”, *Journal of Sound and Vibration*, 229 (2000), 311–327

.

CHAPTER 8 STATUS OF PRIMARY PUBLICATION

ACCEPTED:

L. Wang & L. Dai, “Vibro-acoustic responses of a sandwich panel with aluminum honeycomb core and fabric reinforced graphite face sheets”, *Journal of sandwich structures and materials.*

F. Pan, L. Dai, Y. Hou, M. Du & L. Wang, “Numerical Computation for the Inertial Coupling Vibration System by using PL Method”, *Journal of vibration engineering & technologies.*